AN EXPERIMENTAL INVESTIGATION OF THE ACOUSTIC CHARACTERISTICS OF A VARIETY OF SLOT BAFFLE CONFIGURATIONS FOR TRANSONIC WIND TUNNEL WALLS

N. S. Dougherty, Jr.
ARO, Inc., a Sverdrup Corporation Company

PROPULSION WIND TUNNEL FACILITY
ARNOLD ENGINEERING DEVELOPMENT CENTER
AIR FORCE SYSTEMS COMMAND
ARNOLD AIR FORCE STATION, TENNESSEE 37389

June 1979

Final Report for Period July 1, 1976 — September 30, 1977

Prepared for

NATIONAL AERONAUTICS AND SPACE ADMINISTRATION/ARC
MOFFETT FIELD, CALIFORNIA 94035

NOTICES
When U. S. Government drawings, specifications, or other data are used for any purpose other than a definitely related Government procurement operation, the Government thereby incurs no responsibility nor any obligation whatsoever, and the fact that the Government may have formulated, furnished, or in any way supplied the said drawings, specifications, or other data, is not to be regarded by implication or otherwise, or in any manner licensing the holder or any other person or corporation, or conveying any rights or permission to manufacture, use, or sell any patented invention that may in any way be related thereto.
Qualified users may obtain copies of this report from the Defense Documentation Center.
References to named commerical products in this report are not to be considered in any sense as an indorsement of the product by the United States Air Force or the Government.

This report has been reviewed by the Information Office (OI) and is releasable to the National Technical Information Service (NTIS). At NTIS, it will be available to the general public, including foreign nations.

APPROVAL STATEMENT

This report has been reviewed and approved.

Alexander F. Money

ALEXANDER F. MONEY
Project Manager, Research Division
Directorate of Test Engineering

Approved for publication:

FOR THE COMMANDER

Robert W. Crossley

ROBERT W. CROSSLEY, Lt Colonel, USAF
Acting Director of Test Engineering
Deputy for Operations

REPORT DOCUMENTATION PAGE	READ INSTRUCTIONS BEFORE COMPLETING FORM
1 REPORT NUMBER: AEDC-TR-79-16	2 GOVT ACCESSION NO. / 3. RECIPIENT'S CATALOG NUMBER
4 TITLE (and Subtitle): AN EXPERIMENTAL INVESTIGATION OF THE ACOUSTIC CHARACTERISTICS OF A VARIETY OF SLOT BAFFLE CONFIGURATIONS FOR TRANSONIC WIND TUNNEL WALLS	5 TYPE OF REPORT & PERIOD COVERED: Final Report - July 1, 1976 - September 30, 1977
	6 PERFORMING ORG REPORT NUMBER
7 AUTHOR(s): N. S. Dougherty, Jr., ARO, Inc., a Sverdrup Corporation Company	8 CONTRACT OR GRANT NUMBER(s)
9. PERFORMING ORGANIZATION NAME AND ADDRESS: Arnold Engineering Development Center/DOTR Air Force Systems Command Arnold Air Force Station, Tennessee 37389	10 PROGRAM ELEMENT, PROJECT, TASK AREA & WORK UNIT NUMBERS: Program Element 921E
11 CONTROLLING OFFICE NAME AND ADDRESS: National Aeronautics and Space Administration/ARC Moffett Field, California 94035	12. REPORT DATE: June 1979
	13 NUMBER OF PAGES: 69
14 MONITORING AGENCY NAME & ADDRESS(if different from Controlling Office)	15 SECURITY CLASS (of this report): UNCLASSIFIED
	15a DECLASSIFICATION/DOWNGRADING SCHEDULE: N/A

16 DISTRIBUTION STATEMENT (of this Report)

Approved for public release; distribution unlimited.

17 DISTRIBUTION STATEMENT (of the abstract entered in Block 20, if different from Report)

18 SUPPLEMENTARY NOTES

Available in DDC

19. KEY WORDS (Continue on reverse side if necessary and identify by block number)

disturbances (acoustic)	transonic flow
holes	wind tunnel tests
baffles	walls
configurations	Mach numbers

20 ABSTRACT (Continue on reverse side if necessary and identify by block number)

A parametric study of various slot baffle geometric configurations was performed in an effort to find an improvement to the acoustic characteristics of baffled slotted walls used in the NASA/Ames Research Center transonic wind tunnels. The desired improvement was to reduce the aerodynamic noise generated by these walls. Parameters studied were baffle inclination angle, shape, and depth. A modification to wall samples which effectively

DD FORM 1 JAN 73 1473 EDITION OF 1 NOV 65 IS OBSOLETE

20. ABSTRACT (Continued)

suppressed the noise generated by the baffled slots was a fine-mesh wire screen overlay in combination with baffle inclination angle. The degree of tunnel wall noise suppression achieved in the experiments was a factor of six less than the configuration now in use.

AFSC
Arnold AFB Tenn

ERRATA

AEDC-TR-79-16, June 1979

(UNCLASSIFIED REPORT)

AN EXPERIMENTAL INVESTIGATION OF THE ACOUSTIC CHARACTERISTICS OF A VARIETY OF SLOT BAFFLE CONFIGURATIONS FOR TRANSONIC WIND TUNNEL WALLS

N. S. Dougherty, Jr.
ARO, Inc., a Sverdrup Corporation Company

Propulsion Wind Tunnel Facility
Arnold Engineering Development Center
Air Force Systems Command
Arnold Air Force Station, Tennessee 37389

Equation (4), page 12, of subject report has been revised and is reproduced on the reverse side of this page.

That portion of Section 5.0, CONCLUSIONS AND RECOMMENDATIONS, which appears on page 19 has been revised and is reproduced on the reverse side of this page.

Equation (4)

$$\tilde{p}_{rms} = \left[\frac{1}{T} \int_{o}^{T} [p'(t)]^2 \, dt \right]^{\frac{1}{2}}$$

5.0 CONCLUSIONS AND RECOMMENDATIONS

The significant conclusion from this investigation is that a combination of fine-mesh wire screen overlay with slot baffle inclination was found to be effective in suppressing the type of noise that is generated by baffled transonic wind tunnel slotted walls. The noise was reduced by a factor of six compared to that produced by the . . .

PREFACE

The work reported herein was performed by the Arnold Engineering Development Center (AEDC), Air Force Systems Command (AFSC), for the National Aeronautics and Space Administration (NASA)/Ames Research Center, Moffett Field, California. The experimental results presented herein were obtained by ARO, Inc., AEDC Division (a Sverdrup Corporation Company), operating contractor for the AEDC, AFSC, Arnold Air Force Station, Tennessee. This experimental research was conducted under ARO Project No. P34A-H4A. The manuscript was submitted for publication on January 31, 1979. The AEDC project manager was Alexander F. Money, and the NASA project monitor was F. W. Steinle, Jr.

The author wishes to acknowledge D. W. Sinclair for his assistance in conducting the experiments.

CONTENTS

ILLUSTRATIONS

Figure

Figure | Page

Figure Page

Figure Page

Figure Page

TABLES

1.0 INTRODUCTION

Because aerodynamic noise in the test environment in transonic wind tunnels will significantly affect the location of model boundary-layer transition and possibly affect other boundary-layer characteristics, the NASA/Ames Research Center has become interested in reducing the noise in the Ames 11- by 11-foot and 14- by 14-foot Transonic Wind Tunnels. The source of a discrete frequency disturbance has been isolated to the baffled slots by acoustic measurements made in the tunnels with and without the slots being covered by tape (see Refs. 1, 2, and 3) and by tests of slot samples in the Arnold Engineering Development Center (AEDC) Acoustic Research Tunnel (see Ref. 4).

In the search for an improvement to slot geometry that would eliminate the noise, a parametric study was undertaken in the AEDC-Propulsion Wind Tunnel Facility (PWT) Acoustic Research Tunnel with baffle inclination angle, depth, and shape as the variables. A constraint placed on the study was that any physical modifications should be minimal (no change to the slot number, width, or spacing).

This report describes the experiments performed and the results obtained. Relatively simple modifications of inclined baffles with a wire screen mesh overlay on the airstream side of the tunnel wall were investigated to establish the effects on reducing the noise.

2.0 APPARATUS

2.1 ACOUSTIC RESEARCH TUNNEL

The AEDC-PWT Acoustic Research Tunnel (ART) is a continuous flow, atmospheric indraft tunnel capable of being operated from Mach number 0.1 to 1.1. A schematic diagram of the tunnel is shown in Fig. 1. Acoustic silencers in the diffuser and plenum exhaust ducts, vibration-isolation expansion joints in the diffuser and plenum exhaust ducts and fine-mesh turbulence damping screens and honeycomb in the intake section, combine to provide a low background disturbance level. Tunnel background noise calibration data using smooth, solid test section walls in the ART are given in Fig. 2.

The ART test section is 6 in. square by 24 in. long. The top and bottom wall frames have removable inserts wherein samples of wall sections may be placed for evaluation. The top and bottom walls are capable of divergence from a flexure pitot at the nozzle exit to 0.5-deg maximum in order to compensate for boundary-layer growth on the test section walls. Plenum suction is applied to ventilated wall samples in conjunction with wall divergence at Mach numbers of 0.7 and higher in order to have a uniform axial Mach number distribution through the test section.

2.2 WALL SAMPLES

The slotted walls in the Ames transonic tunnels are formed by structural steel channels laid side by side with a gap between the flanges that form a slot. Two segments of channel pairs with the baffled slot at the center were cut to fit the ART wall frames from an actual piece of wall taken from the Ames 11- by 11-foot Transonic Tunnel. A photograph of one sample is shown in Fig. 3. The slot cross section is shown in Fig. 4. The test configuration in ART was a single full-scale slot along the centerline of the top and bottom walls.

Baffles of varied geometry were interchanged in the slots. The baffle geometries investigated are listed in Table 1. Configuration details are shown in Fig. 5. The axis of bend in the baffles was inclined at the angle θ from the normal to the test section wall in the direction of the flow. The geometric variables were the "zee" and the "semicircular" shape and the baffle depth, D, as defined in Fig. 5. The "zee" configuration at full depth (2.25 in.), normal to the wall (θ = 0) is the presently used configuration in the Ames 11-by 11-foot tunnel and is referred to in this report as the standard baffled slot wall configuration.

Several modifications to the baffle were evaluated. The standard baffled slot wall configurations were covered with 40 by 40 wire-mesh overlay (Fig. 6). Another modification was to drill side-branch orifices (either 0.25-in. or 0.125-in. diam) through the slot flanges in each baffle cell as shown in Fig. 7. The orifices were placed at half-baffle depth (1.125 in.). The standard wall configuration was stuffed with steel wool in the baffle cells, which was held in place by a screen on the back side (away from the flow) of the slot.

2.3 INSTRUMENTATION

A single 0.25-in.-diam Bruel and Kjaer Model 4136 condenser-type microphone, flush-mounted in the tunnel sidewall as shown in Fig. 8, was used to record the fluctuating pressure level in the test section. The fluctuating pressure was measured in a frequency band from approximately 10 Hz to 30 kHz. The microphone signal was measured by a true root-mean-square voltmeter of 1-sec averaging time and on a real-time Fourier spectrum analyzer which incorporated ensemble averaging and variable bandwidth to 20 kHz maximum. The microphone system was calibrated by physical application of a 1-kHz sinusoidal signal of 140 ± 0.5 db (Ref. 0.0002 microbar) using a piston phone.

Static pressure orifices were used in the tunnel sidewall at 1-in. intervals to determine the axial uniformity of the section Mach number. An orifice located at the middle of the test section was used to define tunnel flow conditions. Static pressure in the plenum chamber, p_c, was measured using an orifice located on the forward plenum wall (see Fig. 8). The pressure differential across the wall was then derived from the calculated difference between the test section static pressure and the plenum chamber pressure. The static pressures were measured by a precision strain-gage-type pressure transducer through a sequenced stepping switch.

The tunnel total pressure, p_t, was measured using a pitot probe in the inlet section downstream of the screens and honeycomb. The total temperature was measured using a thermocouple located outside the bellmouth intake.

3.0 PROCEDURE

3.1 DATA ACQUISITION

The procedure for data acquisition was the same as that which had been used in the ART during earlier acoustic studies of other transonic wall samples, as described in Refs. 4 and 5. Measurements were made for each sample configuration as a function of Mach number.

3.2 DATA REDUCTION

The reference wall static pressure, together with the tunnel total pressure, was used to compute Mach number, M_∞, using

$$\frac{p_t}{p_s} = \left(1 + \frac{\gamma - 1}{2} M_\infty^2\right)^{\gamma/\gamma-1} \tag{1}$$

and the dynamic pressure, q_∞, by

$$q_\infty = \frac{\gamma}{2} p_s M_\infty^2 \tag{2}$$

An average wall differential pressure coefficient (between test section and plenum chamber) was computed by

$$C_{p_{wall}} = \frac{p_s - p_c}{q_\infty} \tag{3}$$

where p_c was the measured plenum chamber pressure.

Time-averaged rms fluctuating pressure level recorded on the microphone was computed from instantaneous p'(t) by

$$\tilde{p}_{rms} = \left(\frac{1}{T}\int_0^T \sqrt{p'(t)}\, dt\right) \quad (4)$$

The parameters $\tilde{p}_{rms}$ and q_∞ were then used to compute the fluctuating pressure coefficient ΔC_p, as given by

$$\Delta C_p = \frac{\tilde{p}_{rms}}{q_\infty} \times 100, \text{ percent} \quad (5)$$

The experimental uncertainty in the measurements are:

$\tilde{p}_{rms} \cong \pm 8.5$ percent of reading

$p_s \cong \pm 0.4$ percent of reading

$p_t \cong \pm 0.4$ percent of reading

Computed $M_\infty = \pm 1.0$ percent of reading

Computed $q_\infty = \pm 2.5$ percent of reading

Computed $\Delta C_p = \pm 11$ percent of reading

Resolution of frequencies using the real-time analysis equipment and given in this report was:

for $f \geq 500$ Hz, ± 15 Hz

for $f \leq 500$ Hz, ± 3 Hz

4.0 RESULTS AND DISCUSSION

Three parameters, ΔC_p, predominant frequency composition, and $C_{p_{wall}}$ are the primary performance indicators used in presenting the results. Performance criteria to be used for measuring a successful slot modification were:

1. Significant reduction in noise level (ΔC_p). An order of magnitude reduction was considered highly successful.

2. Absence of predominant frequencies in the slot-generated noise.

3. The differential pressure across the wall ($C_{p_{wall}}$) should be a small positive value not strongly dependent upon Mach number.

The spectral analyses made through this investigation revealed essentially two acoustic modes to be in predominance. The first mode is identified herein as the slot mode, and the second mode (lower frequency than the first mode) is identified herein as the plenum mode. The slot mode was described in Refs. 1 and 4 as an organ pipe standing wave presumed to occur within the slot baffle. This presumption was based on the fact that the same fundamental frequency, 2,700 Hz, was measured for the standard wall configuration in the ART as was measured in the Ames 11- by 11-foot tunnel test section. The plenum mode was identified only in the ART data and is presumed to be peculiar to the slot installation in ART. Hence, it will not be considered in this report in selection of an appropriate slot geometry. For brevity, actual Fourier spectra will not be shown; only the results of scanning the spectra for discrete narrow-band peaks will be presented.

Results of measurements made on the standard wall configuration are presented in the first part of this section. These results include measurements made without baffles and with various noise suppression techniques. Results are then presented of measurements made on inclined baffle configurations that include variations in baffle inclination angle, baffle shape, and baffle depth. The section is concluded by the results of various attempts at suppressing the noise of the inclined baffle configurations.

4.1 STANDARD WALL CONFIGURATION

The standard wall configuration (0-deg inclined, full-depth "zee" baffle) produced noise levels, ΔC_p, which are presented in Fig. 9. Spectral analysis showed predominance of the two slot modes shown in Fig. 10 by closed symbols. The extent of dominance was that the variation in overall ΔC_p' was essentially the variation in amplitude of these two components with M_∞. The slot mode frequencies were nearly constant at 2,700 and 5,400 Hz. Also shown in Fig. 10 are two lower-frequency plenum modes (open symbols) at 180 and 360 Hz, which appeared only when M_∞ was close to 1.0. The wall differential pressure coefficient is shown in Fig. 11. and is slightly positive for all M_∞ which indicates a pressure drop from test section to plenum.

Noise levels measured for the empty slot case (baffles removed) are shown in Fig. 12. The predominant frequencies are shown in Fig. 13. The wall differential pressure coefficient is shown in Fig. 14. In this case. there was no occurrence of 2,700-Hz tones or harmonics thereof, lending evidence to the association of the slot mode with the baffles.

The first attempt at suppressing the slot mode in the standard wall configuration was to use the side-branch orifices shown in Fig. 7. The idea employed here was that a

vent at half-baffle depth from each baffle cell through the slot flange would detune the baffle from its tendency to produce a standing wave. Results are shown in Fig. 15 for the 1/8-in. and 1/4-in.-diam orifices tried. The degree of noise suppression was only slight, and the vent concept was abandoned.

The second attempt at noise suppression was to use the wire screen overlay shown in Fig. 6. The results with wire screen overlay in terms of ΔC_p are shown in Fig. 16. Wire screen alone was not effective in suppressing the slot mode. When steel wool stuffing was placed inside the baffle cells with wire screen at the top and bottom of the slot to retain the steel wool, the slot tones were effectively suppressed as shown in Fig. 16. The tones disappeared from the spectra, and ΔC_p closely approached the background level with solid test section walls. The idea in using steel wool stuffing was to break up the presumed standing wave in the slot baffle. The results indicate that the steel wool was effective. The wall differential pressure coefficients for the cases of wire screen and wire screen plus steel wool are shown in Fig. 17. The steel wool caused an excessive pressure drop across the wall which was considered inappropriate for application to an actual wind tunnel.

4.2 INCLINED BAFFLE CONFIGURATIONS

The matrix of tests performed to show effects of varied baffle geometry is shown in Table 2. The maximum values of ΔC_p and $C_{p_{wall}}$ and the Mach number at which a maximum occurred are listed in Table 2.

4.2.1 Baffle Inclination Angle

The results obtained for the full-depth, "zee" baffle configuration with baffle inclination angle θ = 60 deg are shown in Fig. 18 in terms of ΔC_p versus M_∞. The predominant frequencies are shown in Fig. 19. The wall differential pressure coefficient is shown in Fig. 20. There was a shift in the slot mode frequencies to as low as 730 Hz at M_∞ = 0.8 for the lowest-frequency tone. Slot mode frequencies decreased with increasing M_∞ as seen in Fig. 19. The wall differential pressure coefficient, Fig. 20, was negative over most of the range of M_∞, indicating some pressure recovery to have occurred across the inclined-baffle slot. This pressure differential became smaller when plenum suction was added for $M_\infty \geq 0.7$.

At θ = 45 deg for the "zee" baffle shape, full depth, there was an increase in ΔC_p as M_∞ approached 1.0 as shown in Fig. 21. The slot mode appeared only at M_∞ = 0.7, 0.95, and 1.0 in this case as shown in Fig. 22. The wall differential pressure coefficient was negative over the full Mach number range, and lower in magnitude than the θ = 60-deg case as shown in Fig. 23.

At θ = 30 deg, ΔC_p did not reach values as large as in the θ = 45-deg case as shown in Fig. 24. The slot mode was present at $M_\infty \geq 0.5$ as shown in Fig. 25. The slot mode frequencies were again virtually constant, as in the normal (θ = 0) case, and at the same levels of approximately 2,650 and 5,300 Hz. The wall differential pressure coefficient was extremely small for θ = 30 deg as seen in Fig. 26, going slightly positive with the application of suction for $M_\infty \geq 0.8$.

At θ = 15 deg, ΔC_p was still large in amplitude, although lower than the standard normal baffle case (Fig. 9) as seen in Fig. 27. The slot mode was again present as shown in Fig. 28, occurring for $M_\infty \geq 0.5$ at approximately 2,650 and 5,300 Hz. The wall differential pressure coefficient was still small as seen in Fig. 29.

Reversing the direction of the 15-deg inclined baffle to θ = -15 deg produced a significant reduction in ΔC_p to 1.4 percent maximum as shown in Fig. 30. As seen in Fig. 31, the occurrence of the two modes with sufficient amplitude to be perceived above the background spectra was limited to only a narrow range of Mach numbers. The wall differential pressure coefficient was positive over the full range of M_∞ and slightly increased as shown in Fig. 32.

In summary, for the full-depth "zee" baffle tests with varied inclination angle, inclination to θ = 60 deg altered the nature of the slot mode to lower frequencies and reduced the overall amplitude in ΔC_p below that which occurred for the standard baffle. Furthermore, the wall differential pressure coefficient indicated presssure recovery instead of loss for the 60-deg inclined baffle. At θ = 45 deg, the slot mode was almost nonexistent except near M_∞ = 1.0 where the combination of both slot and plenum modes produced a ΔC_p greater than the standard baffle configuration. At θ = 30 and 15 deg, the slot mode occurred at essentially the same frequency levels as the standard baffle case. With slightly negative baffle inclination angle, θ = -15 deg, there was significant reduction in ΔC_p with suppression of the occurrence of the slot mode; however, the levels of ΔC_p for this case were still much higher than the levels achieved with steel wool in the standard baffle.

4.2.2 Baffle Shape

Selected "semicircular" baffle (Fig. 5) shape data for the full-depth case will be presented. Only ΔC_p will be shown, Fig. 33, for the θ = 60-deg case. It is seen in Fig. 33 that there is no advantage to the "semicircular" shape at θ = 60 deg over the "zee" shape since ΔC_p was increased above the levels in Fig. 18. At θ = 45 deg, ΔC_p was still high as shown in Fig. 34; predominant frequencies are shown in Fig. 35. At θ = 30 deg, ΔC_p was still large as seen in Fig. 36; the slot mode frequencies shifted to slightly higher

than those of the "zee" shape as seen Fig. 37; and the wall pressure coefficient shows a recovery for $M_\infty < 0.6$ and a drop for $M_\infty \geq 0.6$ in Fig. 38. At θ = 15 deg, the ΔC_p amplitudes were still large as seen in Fig. 39; the slot mode frequency became constant at approximately 2,700 and 5,400 Hz as seen in Fig. 40; and the wall differential pressure coefficient showed a drop across the wall in Fig. 41.

In summary, the data for the "semicircular" shape at full-baffle depth show no particular advantage over the "zee" baffle shape. The acoustic phenomena taking place were essentially the same for both shapes and there was no reduction in ΔC_p. Because a "semicircular"-shaped baffle was found to be more difficult to manufacture than a "zee"-shaped baffle, there is no basis to recommend its use over the "zee"-shaped baffle for full-depth baffle configurations.

4.2.3 Baffle Depth

A lower level of ΔC_p was found to occur for the 60-deg inclined, half-depth "zee" baffle than for the standard baffle (Fig. 9) as seen in Fig. 42. The slot mode occurred at $M_\infty \geq 0.7$, as seen in Fig. 43, indicating some change in the slot flow conditions associated with plenum suction application at M_∞ = 0.7. Surprisingly, a lower - not higher - slot mode frequency occurred for the half-depth baffled slot, 1,450 Hz at M_∞ = 0.9. The wall differential pressure coefficient showed a relatively large pressure recovery for $M_\infty \leq 0.6$ which was almost nullified by plenum suction application as seen in Fig. 44.

Still lower amplitudes of ΔC_p were found for the half- depth "zee" baffle at θ = 45 deg as shown in Fig. 45. The slot mode had shifted upward in frequency to 1,750 to 1,900 Hz and 4,200 Hz as seen in Fig. 46. The degree-of-pressure recovery across the wall was reduced at θ = 45 deg compared to that at θ = 60 deg, becoming positive with plenum suction application as seen in Fig. 47.

At θ = 30 deg for the half-depth "zee" baffle, a large spike in ΔC_p versus M_∞ occurred at M_∞ = 0.5 as shown in Fig. 48. The slot mode was amplified to ΔC_p = 6.8 percent at M_∞ = 0.5 as seen in Fig. 49. (With the large amplitude, there was increased distortion to the slot mode with a strong third harmonic in addition to the first two.) The wall differential pressure coefficient was essentially zero for $M_\infty \leq 0.6$ and positive with plenum suction at $M_\infty \geq 0.7$ as seen in Fig. 50.

At θ = 15 deg for the half-depth "zee" baffle, the levels of ΔC_p were about the same as those at θ = 60 deg as seen in Fig. 51. The frequency composition of the noise was considerably different, there being a varied assortment of higher-order harmonics of

the plenum mode and prevalence of the higher harmonic of the slot mode as seen in Fig. 52. The wall differential pressure coefficient was about the same as for the θ = 30-deg case as seen in Fig. 53.

Inclination of the half-depth "zee" baffle to θ = -15 deg produced a reduction in ΔC_p as seen in Fig. 54 to about the same level as that for the θ = -15 deg, full-depth baffle case in Fig. 30, the maximum level being 1.25 percent. In this case, detection of predominant frequencies was barely possible above the background spectra at the Mach numbers shown in Fig. 55. The wall differential pressure coefficient remained positive over the full Mach number range as shown in Fig. 56.

Changing the baffle geometry from "zee" to "semicircular" for the half-depth case at θ = 60 deg produced a substantial increase in ΔC_p as seen in Fig. 57. The ART plenum mode was prevalent, producing the large amplitude ΔC_p at the lower Mach numbers as seen in Fig. 58. The slot mode occurred only for $M_\infty \geq 0.6$. The harmonic array of frequencies decreased with increasing M_∞ in a clearly established pattern, the lowest slot mode frequency being 750 Hz at M_∞ = 0.75. Large pressure recovery across the wall was indicated by $C_{P_{wall}}$, which was nullified by the application of plenum suction as seen in Fig. 59.

For the θ = 45-deg. "semicircular", half-depth baffle configuration, ΔC_p was again high relative to the "zee"- shaped baffle (Fig. 45) as seen in Fig. 60. Resonance occurred over most of the range of M_∞ as seen in Fig. 61. The differential pressure coefficient across the wall became gradually less negative as M_∞ was increased as seen in Fig. 62.

Noise results obtained with the θ = 30-deg, "semicircular", half-depth baffle configuration in terms of ΔC_p are shown in Fig. 63. Again, ΔC_p was higher than the "zee"-shaped baffle results except near the spike at M_∞ = 0.5 shown in Fig. 48. The predominant frequencies are shown in Fig. 64. The wall differential pressure coefficient is shown in Fig. 65.

For the θ = 15-deg. "semicircular", half-depth baffle configuration, ΔC_p was slightly higher than the "zee"-shaped baffle results (Fig. 51) as seen in Fig. 66. The predominant frequencies are shown in Fig. 67. The wall differential pressure was shifted toward the positive as seen in Fig. 68.

In summary, these tests of the half-depth baffle revealed higher levels of ΔC_p for the "semicircular" shape than for the "zee" shape. The half-depth "zee" configuration produced lower levels of ΔC_p than the standard configuration, but the frequencies of the slot mode were lowered.

4.3 TRIAL MODIFICATIONS FOR INCLINED BAFFLES

Three modifications to the inclined baffles were tried: one was to simply recess the θ = 60-deg, full-depth "zee" baffle 1/4 in. below the wall surface, another was to stack two half-depth "zee" baffles with the upper section at θ = 45 deg and the lower section at θ = -30 deg. and the third was to place wire screen overlay on the inclined full-depth "zee" baffles.

4.3.1 Recessed "Zee" Baffle

Recessing the θ = 60-deg, full-depth, "zee"-type baffle by 1/4 in. below the wall surface provided no real improvement in terms of noise reduction compared, for example, to the nonrecessed results in Fig. 18. The noise levels are shown in Fig. 69. The predominant frequencies are shown in Fig. 70. The ART plenum mode was predominant in all spectra. The slot mode was detectable only at M_∞ = 0.9. The wall differential pressure coefficient, shown in Fig. 71, was shifted slightly toward less negative values for $M_\infty \leq 0.7$, relative to the nonrecessed results shown in Fig. 20. At M_∞ = 0.9, $C_{p_{wall}}$ increased to +0.2, which is excessively high.

Although the recessing concept might have been tried on samples of different inclination angle and depth, or even on the "semicircular" shape, these results provided no sign of encouragement, and this approach at noise suppression was abandoned.

4.3.2 Bidirectional Inclined Baffle

The stacking of two half-depth baffles, one inclined with the flow and the other inclined against the flow, was tried as a noise suppression technique. The selection of angles was arbitrary, θ = 45 deg for the upper section and θ = -30 deg for the lower section.

The results were not encouraging as seen in the noise levels in Fig. 72. Both plenum and slot modes were present, slot mode in Fig. 73. The wall differential pressure coefficient is shown in Fig. 74. The bidirectional baffle configuration could possibly be optimized, but there was no sign in the test to indicate that the idea was worthwhile to pursue.

4.3.3 Wire Screen Overlay on Inclined Baffles

Having had success with wire screen overlay at noise suppression in other types of transonic walls (see Ref. 4), wire screen overlay was tried on inclined baffles. The full-depth "zee"-type baffles were selected for these tests.

Noise levels from the θ = 60-deg, full-depth, "zee"-type baffles with 40 by 40 mesh wire screen overlay are shown in Fig. 75. The maximum level of ΔC_p was 0.64 percent at M_∞ = 0.8, and the levels at all M_∞ compared extremely well with the solid wall background levels (taken from Fig. 2). No predominant peaks of any consequence could be found in the spectra. An excessive value of $C_{p_{wall}}$ occurred when plenum suction was added at M_∞ = 0.8 and 0.9, $C_{p_{wall}}$ = 0.24, as seen in Fig. 76.

Changing the baffle inclination to θ = 45 deg produced essentially identical low levels of ΔC_p as seen in Fig. 77. Again, the spectra were free of any peaks. The differential pressure coefficient was $C_{p_{wall}}$ = 0.06 maximum at M_∞ = 0.9, as seen in Fig. 78, much lower than that which had occurred at θ = 60 deg.

When the baffle angle was changed to θ = 30 deg, the degree-of-noise suppression was equally as good as at the greater angles as seen in Fig. 79. There were no spectral peaks. The wall differential pressure coefficient was slightly increased to $C_{p_{wall}}$ = 0.12 at M_∞ = 0.9 as seen in Fig. 80.

At θ = 15 deg, there was still very effective noise suppression as seen in Fig. 81. Still there were no spectral peaks. The wall differential pressure coefficient reached $C_{p_{wall}}$ = 0.09 at M_∞ = 0.9 as seen in Fig. 82.

In summary, the wire screen overlay gave very effective noise suppression for "zee"-type baffles of full depth, inclined at all angles from θ = 60 to 15 deg. The excessively high pressure drop across the wall, $C_{p_{wall}}$ = 0.24. at θ = 60 deg is a basis for exclusion of the 60-deg inclined baffle. The preferable range in baffle inclination angle with wire screen overlay, therefore, lies in the range 45 deg $\geq \theta \geq$ 15 deg.

To pick one baffle configuration, the θ = 45 deg with wire screen overlay is probably the optimum of those investigated here because of the low $C_{p_{wall}}$ values which were not much different from those of the standard wall configuration (compare Fig. 78 with Fig. 11). A second reason for this choice of θ = 45 deg is that this was the angle without screen overlay at which the resonant frequencies had the least occurrence over the Mach number range.

5.0 CONCLUSIONS AND RECOMMENDATIONS

The significant conclusion from this investigation is that a combination of fine-mesh wire screen overlay with slot baffle inclination was found to be effective in suppressing the type of noise that is generated by baffled transonic wind tunnel slotted walls. The degree-of-noise reduction obtained was a factor of six less than that produced by the

standard wall configuration and had no predominant resonant frequencies. The "zee"-shaped baffle of depth equal to that of the normal baffle used in the NASA/Ames 11- by 11-foot transonic tunnel with a baffle inclination angle of 45 deg appears to be the optimal choice. This configuration produced low positive wall pressure differentials not materially different from those of the currently employed slotted wall. The wire screen overlay was not effective in suppressing the noise in the standard wall configuration (0-deg inclined baffles) presently used at Ames.

The present investigation was performed with nonscale boundary layers and plenum chamber size relative to the slot dimensions. An acoustic verification test should be performed in a properly scaled experiment, and wall interference testing should be performed for a slotted wall with the modified baffle geometry before proceeding with modification to a full-scale wind tunnel.

REFERENCES

1. Dougherty, N. S., Jr. and Steinle, F. W., Jr. "Transition Reynolds Number Comparisons in Several Major Transonic Tunnels." AIAA Paper No. 74-627, Presented at the AIAA 8th Aerodynamic Testing Conference, Bethesda, Maryland, July 8-10, 1974.

2. Whitfield, J. D. and Dougherty, N. S., Jr. "A Survey of Transition Research at AEDC." AEDC-TR-77-52 (ADA041740), July 1977; Also Presented at the AGARD Fluid Dynamics Panel Symposium on Laminar-Turbulent Transition, Lyngby, Denmark, May 2-4, 1977, AGARD CP No. 224.

3. Dods, J. B. and Hanly, R. D. "Evaluation of Transonic and Supersonic Wind Tunnel Background Noise and Effects on Surface Pressure Fluctuation Measurements." AIAA Paper No. 72-1004, Presented at the AIAA 7th Aerodynamic Testing Conference, Palo Alto, California, September 1972.

4. Dougherty, N. S., Jr. "A Study of Acoustic Disturbances and Means of Suppression in Ventilated Transonic Wind Tunnel Walls." AEDC-TR-77-67 (ADA045347), October 1977.

5. Dougherty, N. S., Jr., Anderson, C. F., and Parker, R. L., Jr. "An Experimental Investigation of Techniques to Suppress Edgetones from Perforated Wind Tunnel Walls." AEDC-TR-75-88 (ADA013728), August 1975; Also AIAA Paper No. 76-50, Presented at the AIAA 14th Aerospace Sciences Meeting, Washington, D. C., January 26-28, 1976.

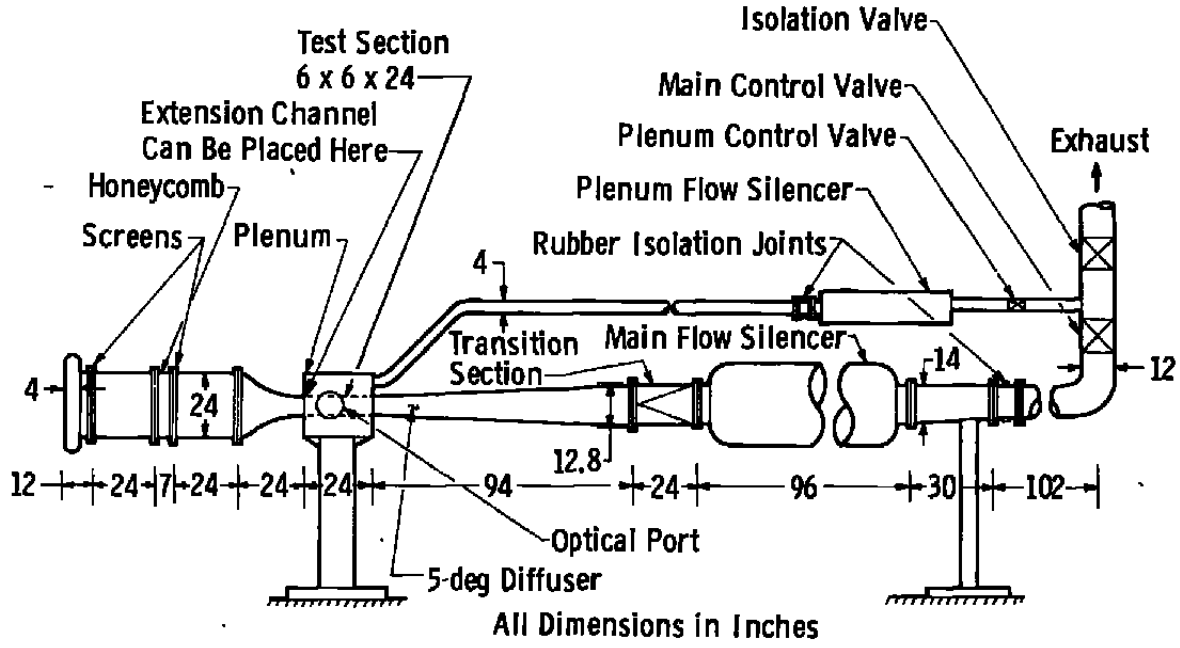

a. Overall layout

Figure 1. Acoustic Research Tunnel.

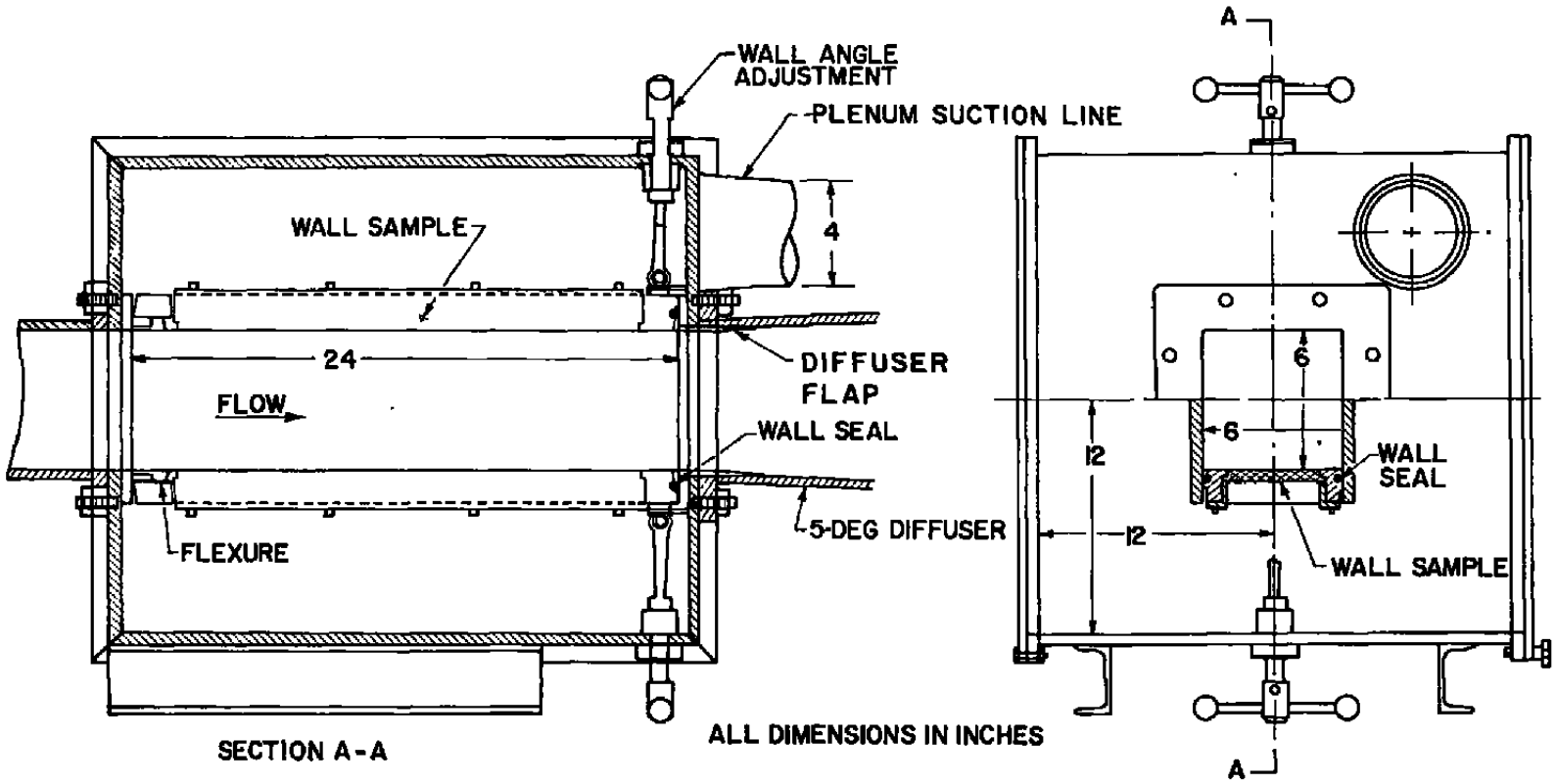

b. Test section and plenum details

Figure 1. Concluded.

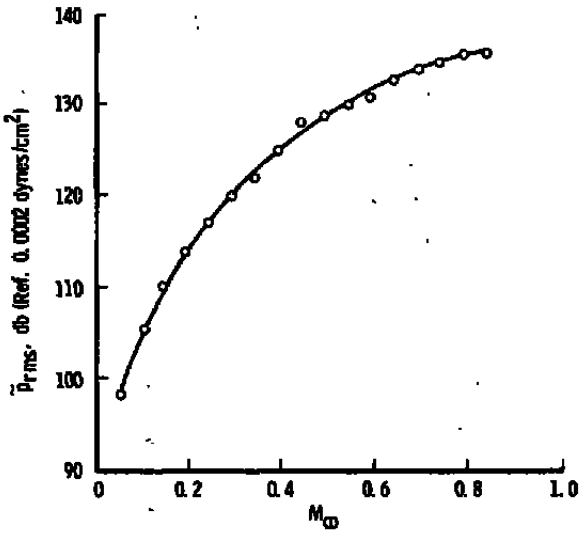

a. Amplitudes

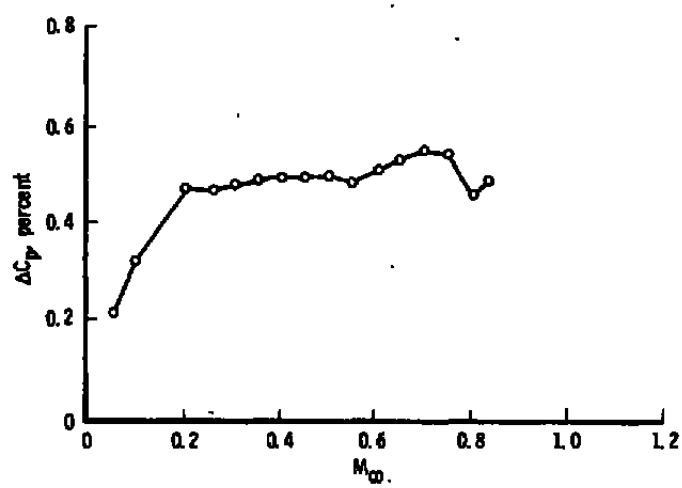

b. Normalized amplitudes

Figure 2. Solid wall background noise.

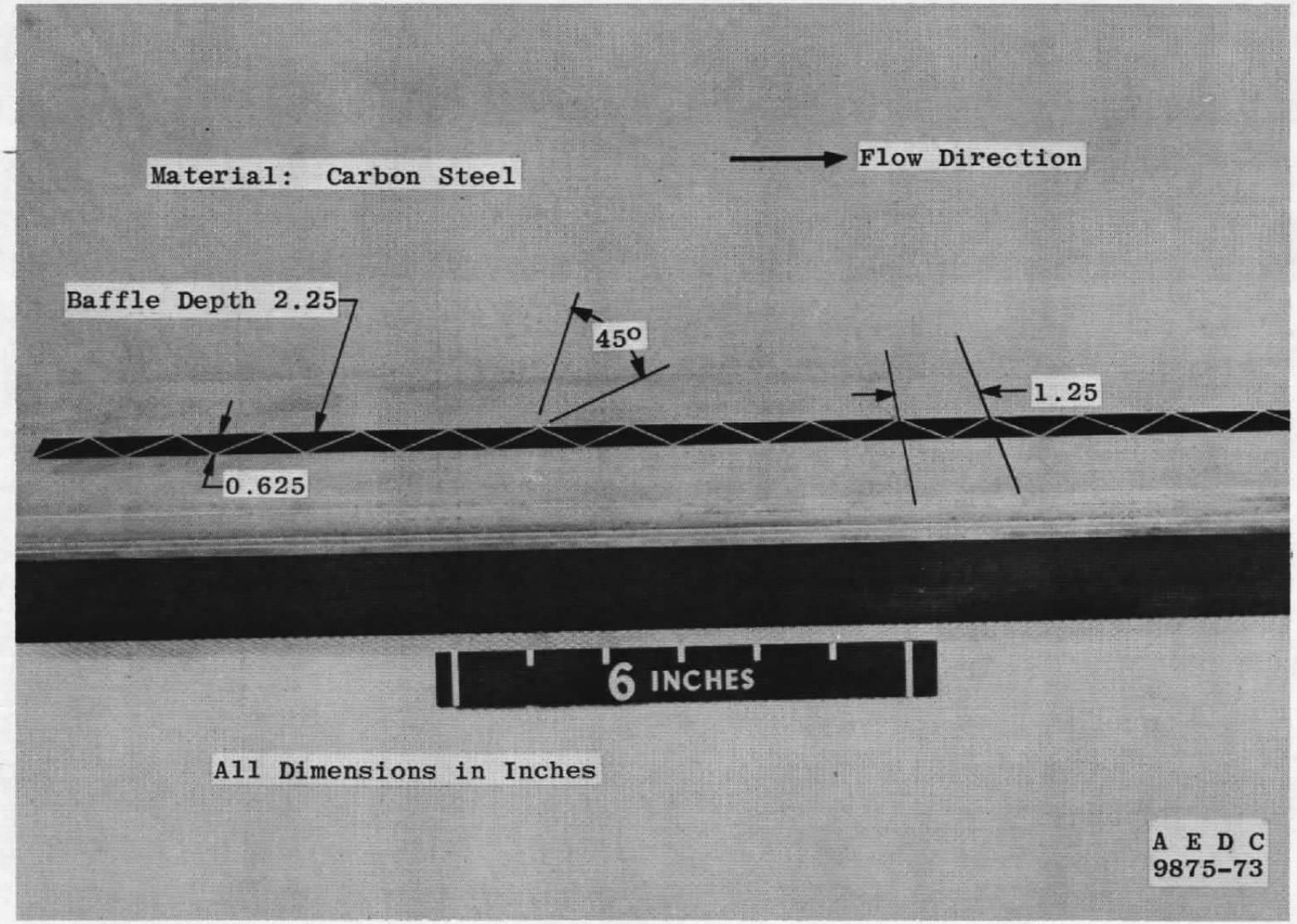

Figure 3. Standard baffled slot.

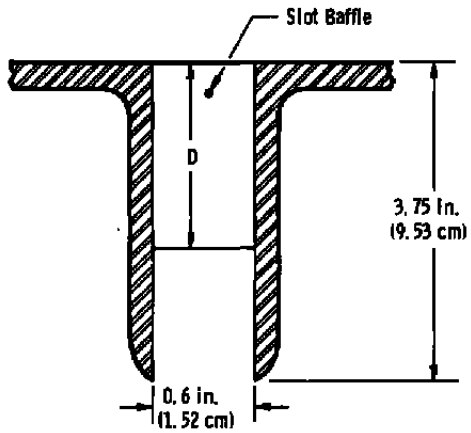

Figure 4. Slot cross-section details.

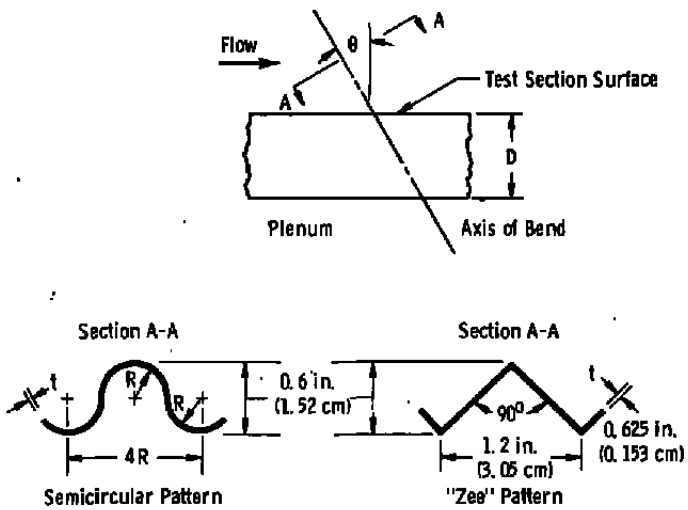

Figure 5. Baffle geometry.

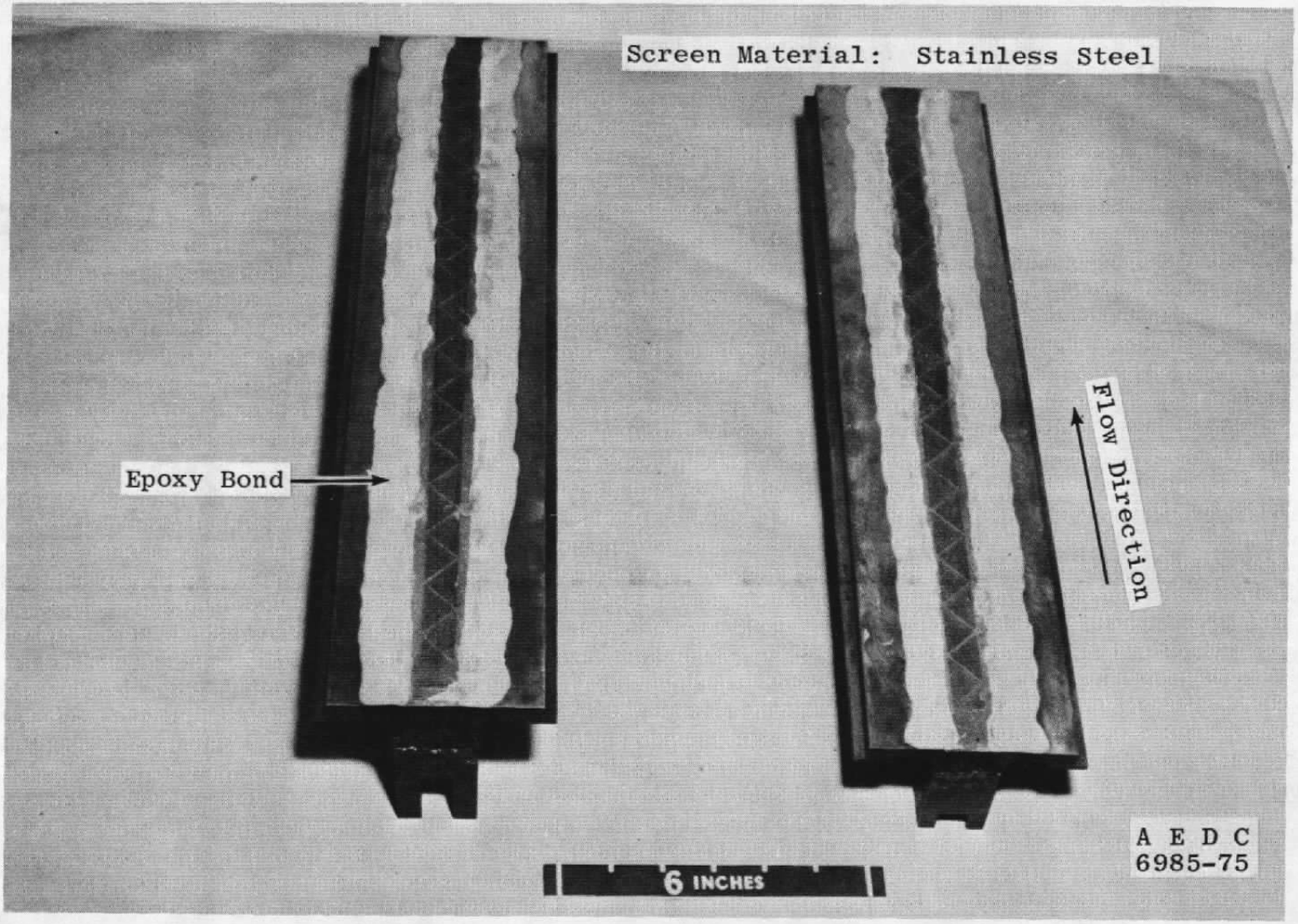

Figure 6. Wire screen overlay installation on the standard baffled slot wall configuration.

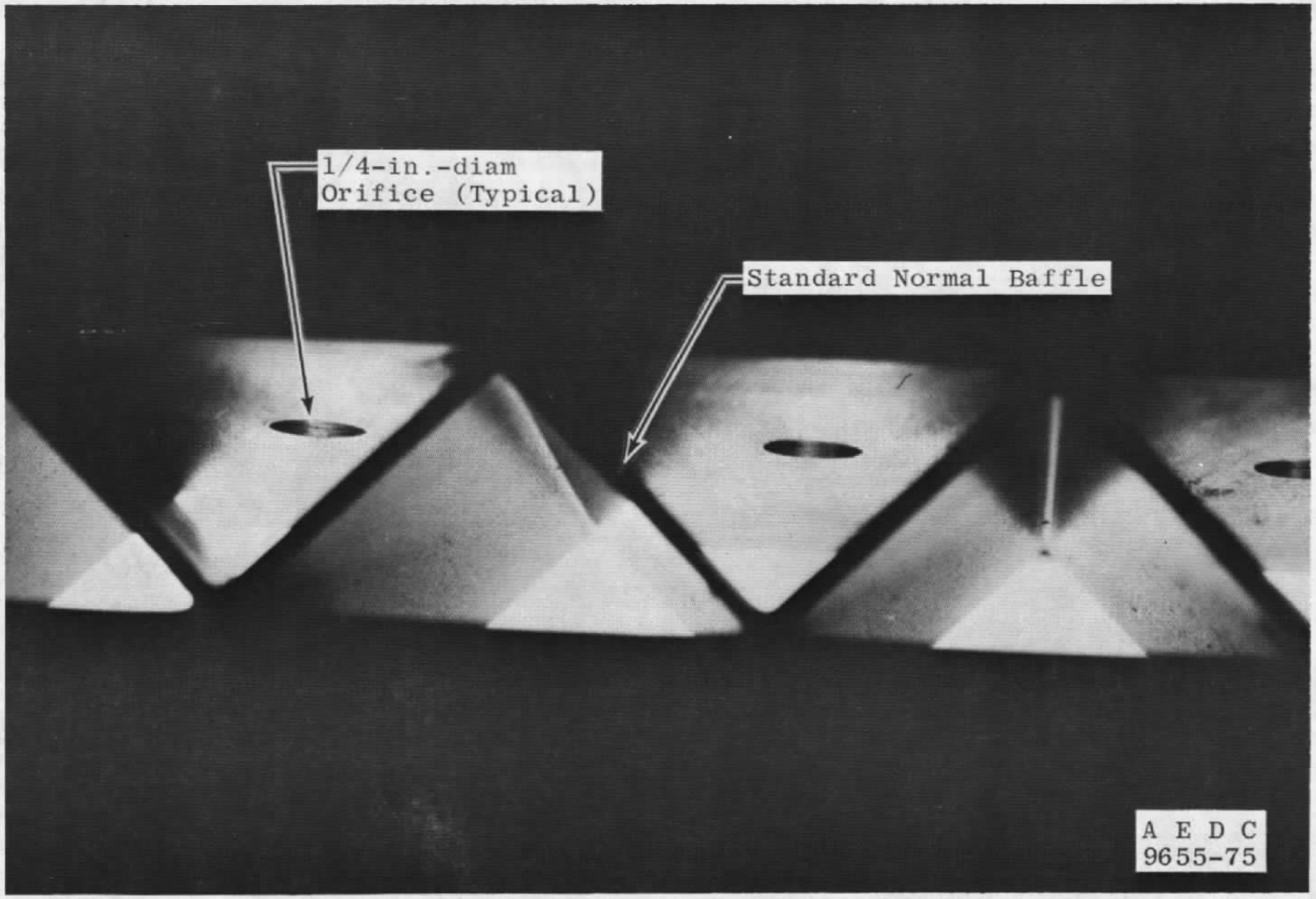

Figure 7. Side branch orifices in standard baffled slots.

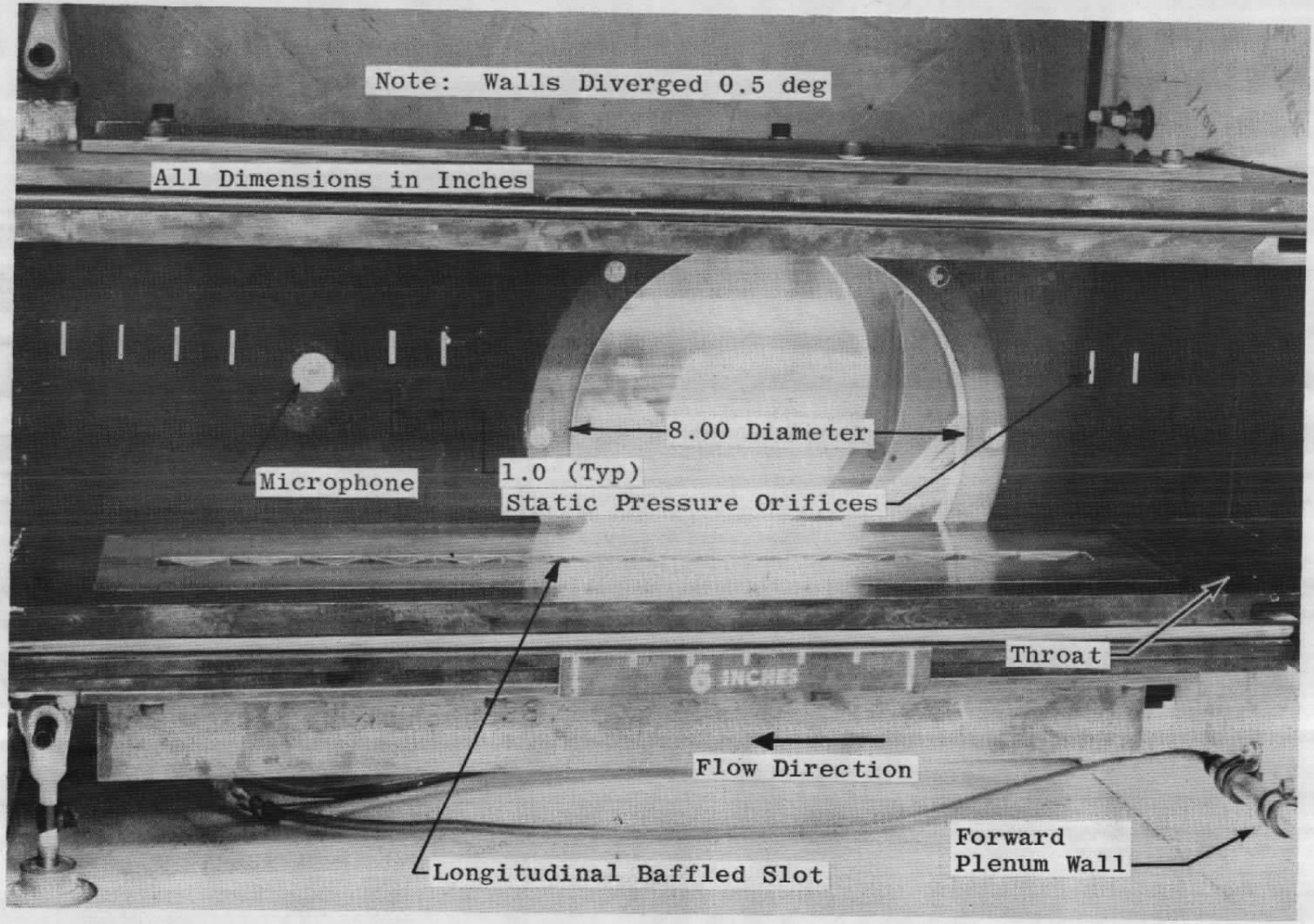

a. Test section arrangement

Figure 8. Instrumentation location details.

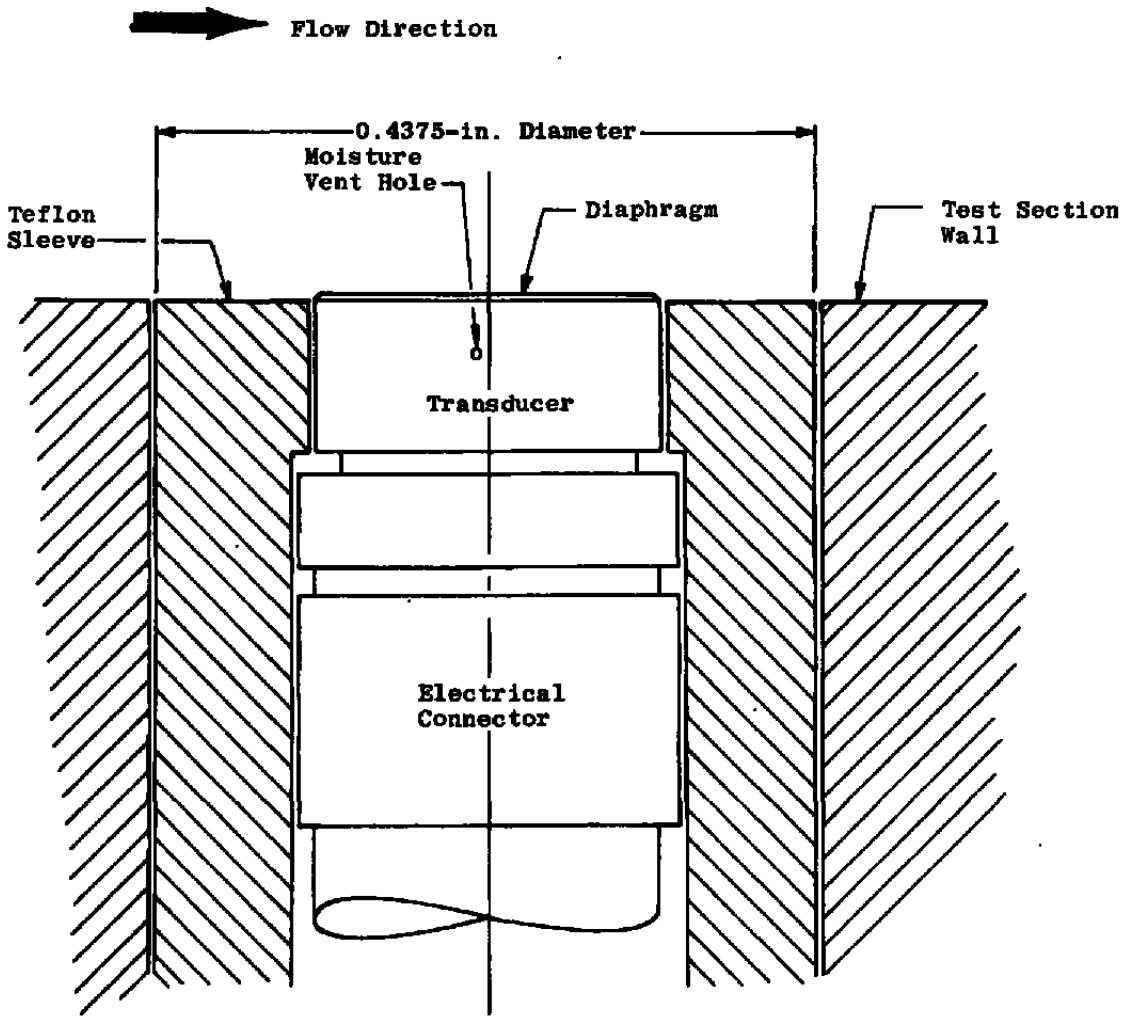

b. Microphone installation details
Figure 8. Concluded.

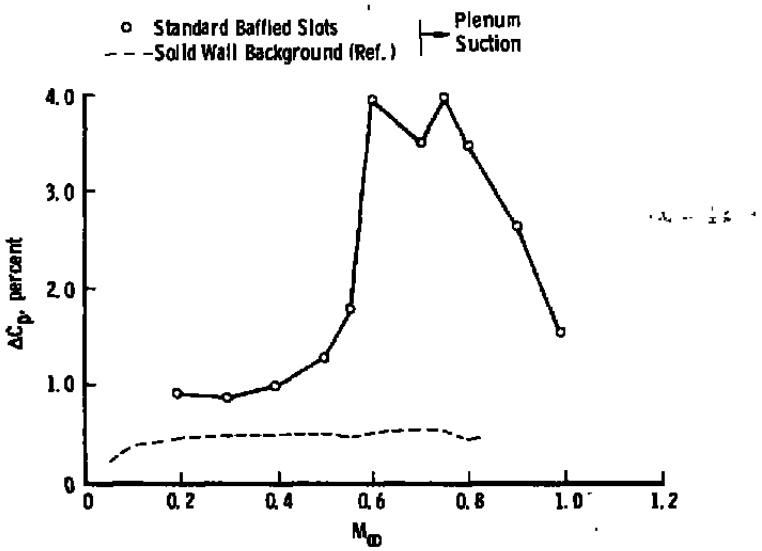

Figure 9. Noise levels from the standard baffled slots.

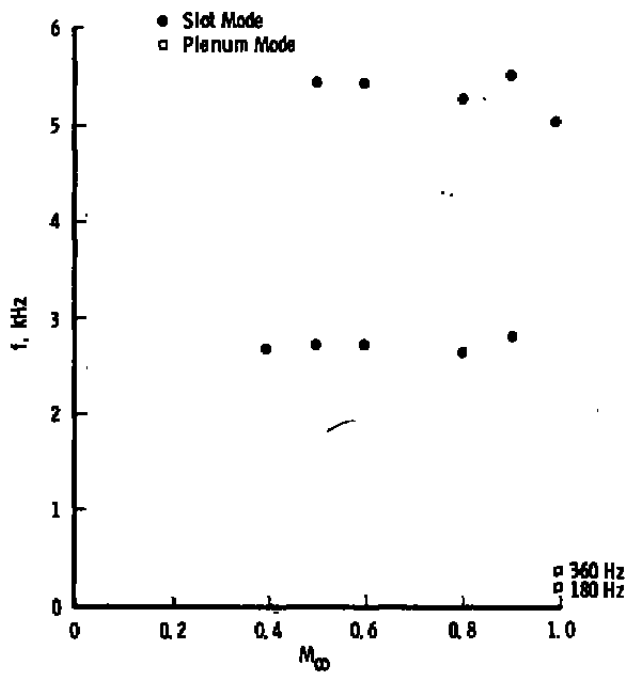

Figure 10. Predominant frequencies from the standard baffled slots.

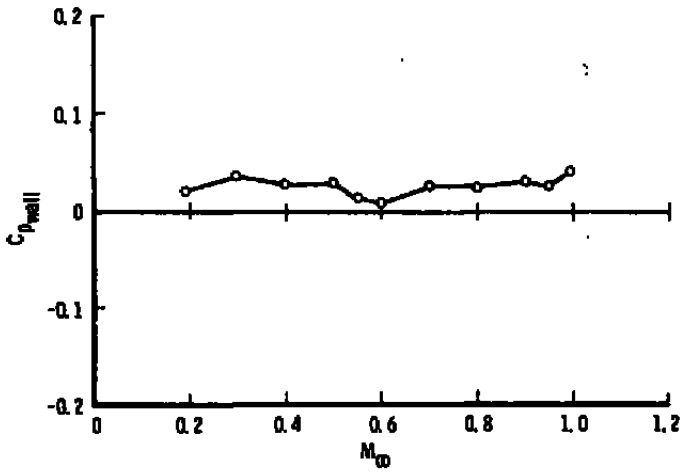

Figure 11. Wall pressure differential with the standard baffled slots.

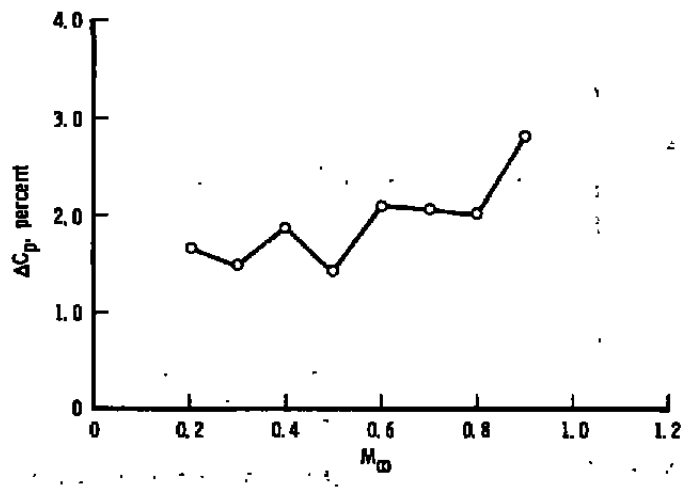

Figure 12. Noise levels from the empty slots.

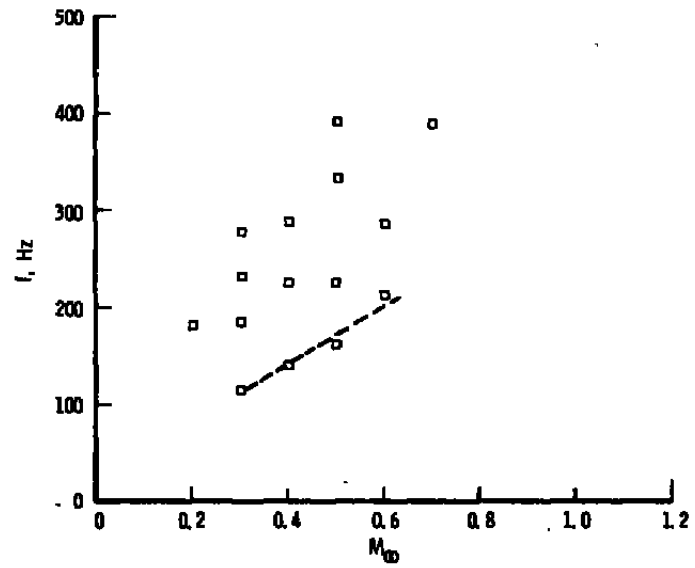

Figure 13. Predominant frequencies from the empty slots.

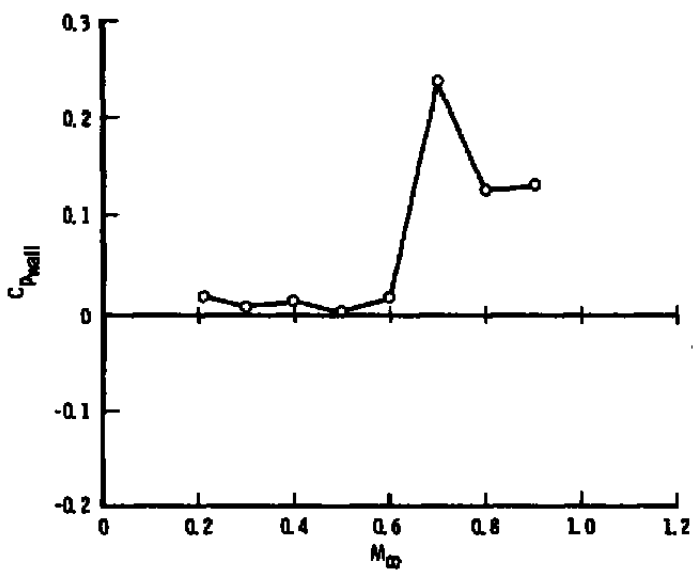

Figure 14. Wall differential pressure coefficient with the empty slots.

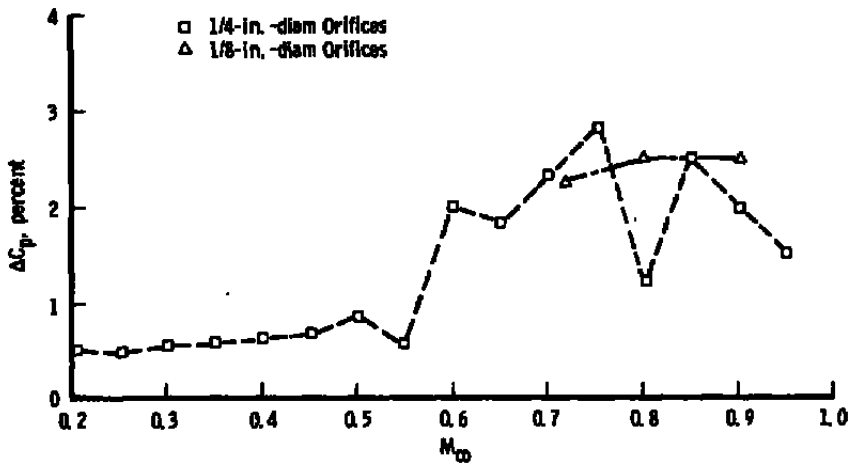

Figure 15. Noise levels with orifices in the standard baffled slots.

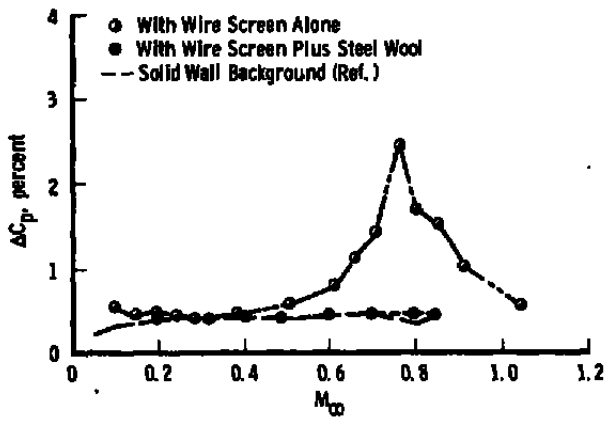

Figure 16. Noise levels with wire screen and with steel wool stuffing in the standard baffled slots.

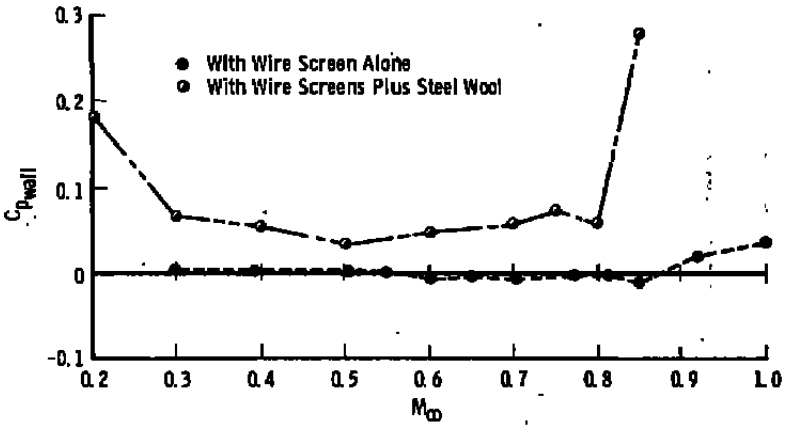

Figure 17. Wall differential pressure coefficient with wire screen and with steel wool stuffing in the standard baffled slots.

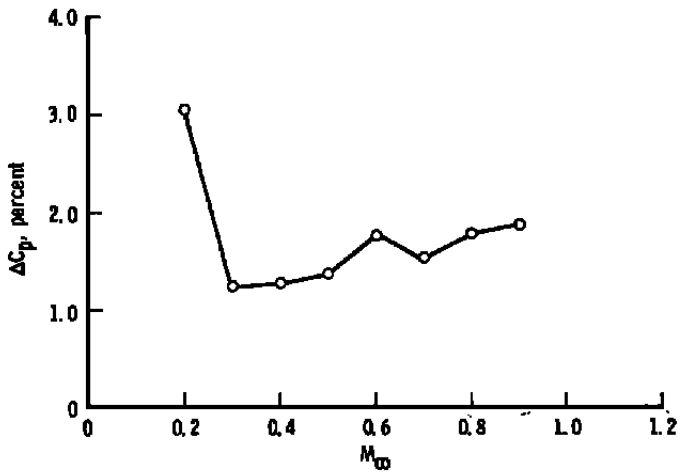

Figure 18. Noise levels from full-depth "Zee" baffle slots inclined 60 deg.

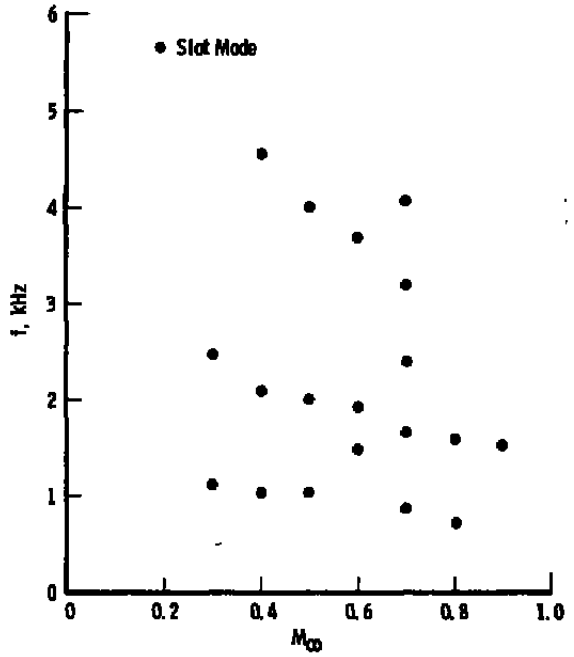

Figure 19. Predominant frequencies from full-depth "Zee" baffle slots inclined 60 deg.

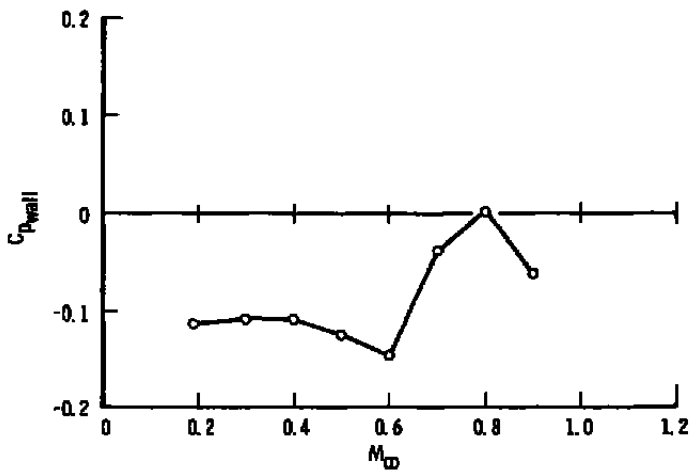

Figure 20. Wall differential pressure coefficient with full-depth "Zee" baffle slots inclined 60 deg.

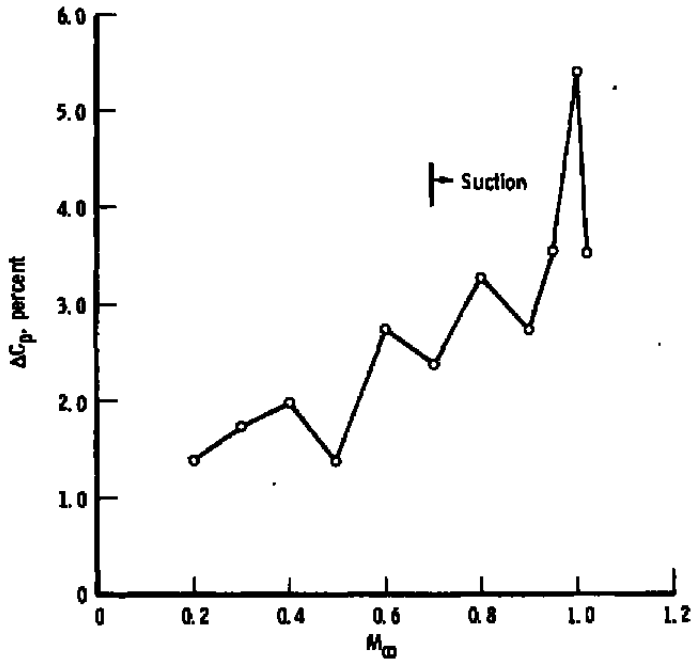

Figure 21. Noise levels from full-depth "Zee" baffle slots inclined 45 deg.

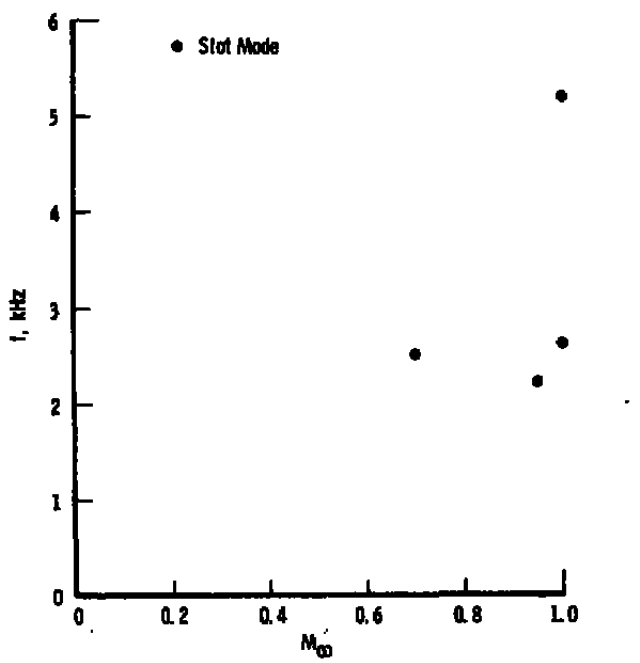

Figure 22. Predominant frequencies from full-depth "Zee" baffle slots inclined 45 deg.

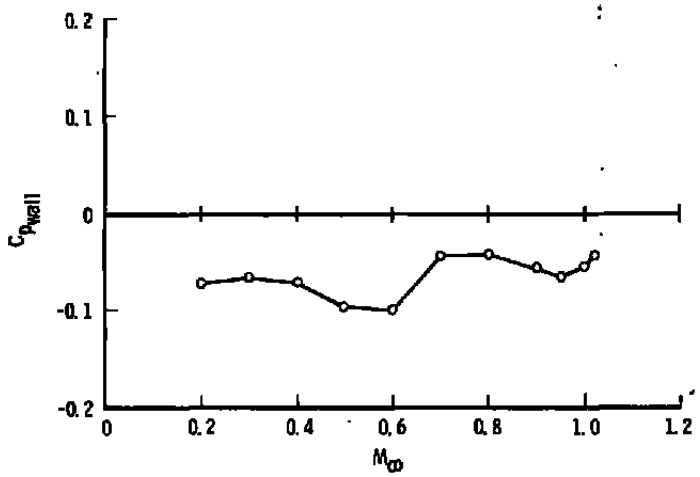

Figure 23. Wall differential pressure coefficient with "Zee" baffle slots inclined 45 deg.

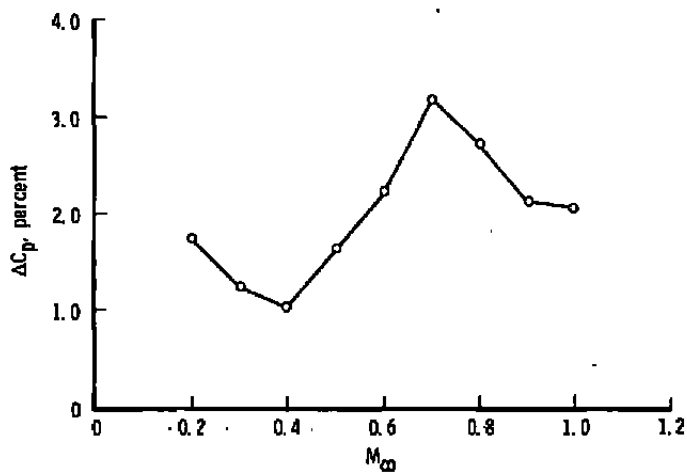

Figure 24. Noise levels from full-depth "Zee" baffle slots inclined 30 deg.

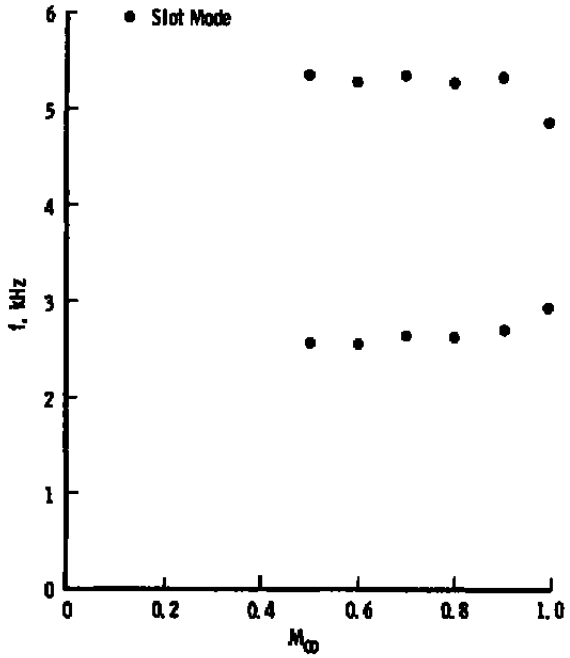

Figure 25. Predominant frequencies from full-depth "Zee" baffle slots inclined 30 deg.

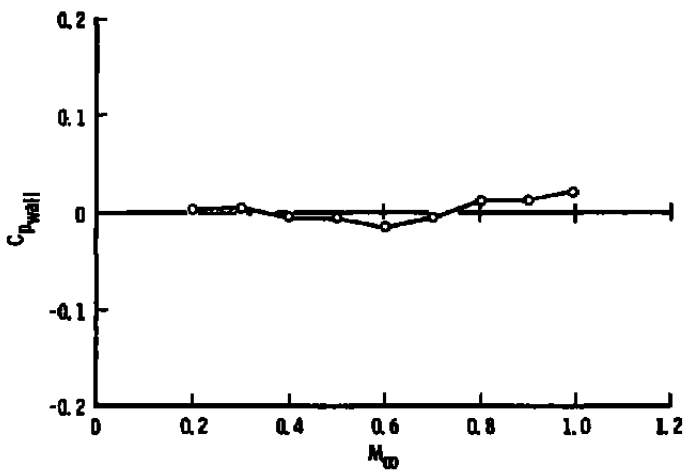

Figure 26. Wall differential pressure coefficient with "Zee" baffle slots inclined 30 deg.

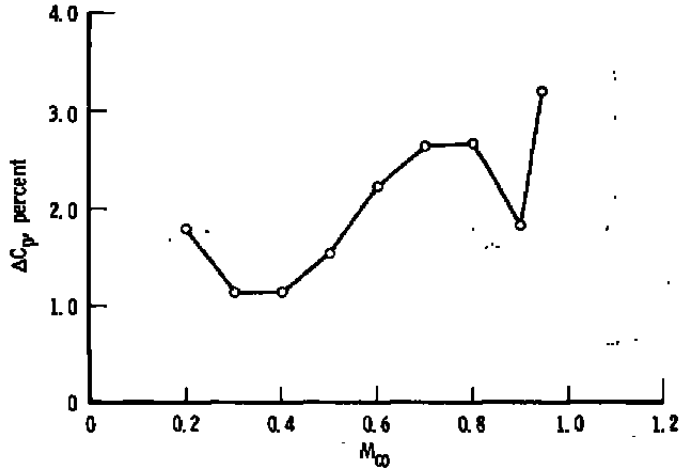

Figure 27. Noise levels from full-depth "Zee" baffle slots inclined 15 deg.

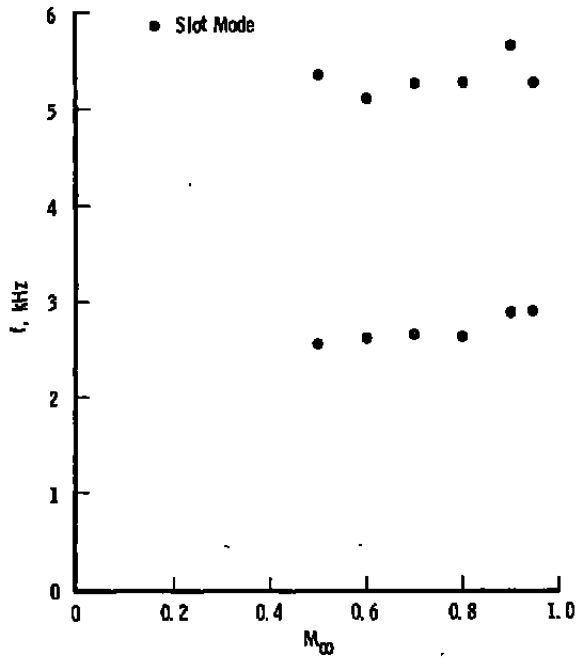

Figure 28. Predominant frequencies from full-depth "Zee" baffle slots inclined 15 deg.

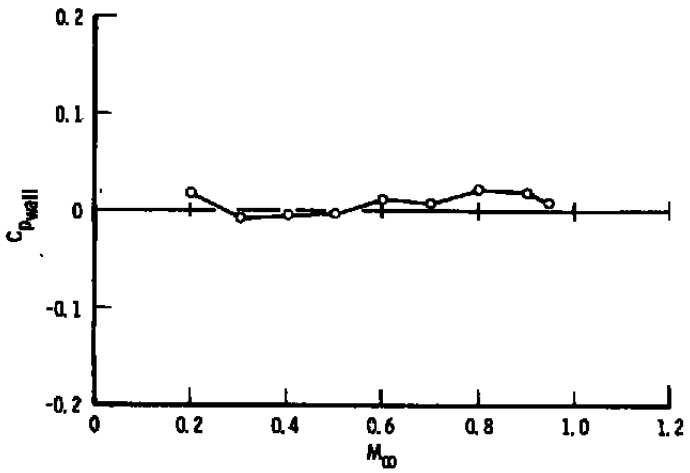

Figure 29. Wall differential pressure coefficient with full-depth "Zee" baffle slots inclined 15 deg.

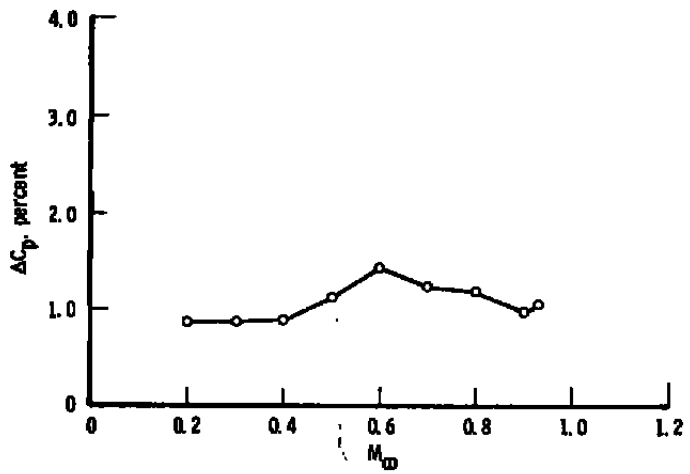

Figure 30. Noise levels from full-depth "Zee" baffle slots inclined -15 deg.

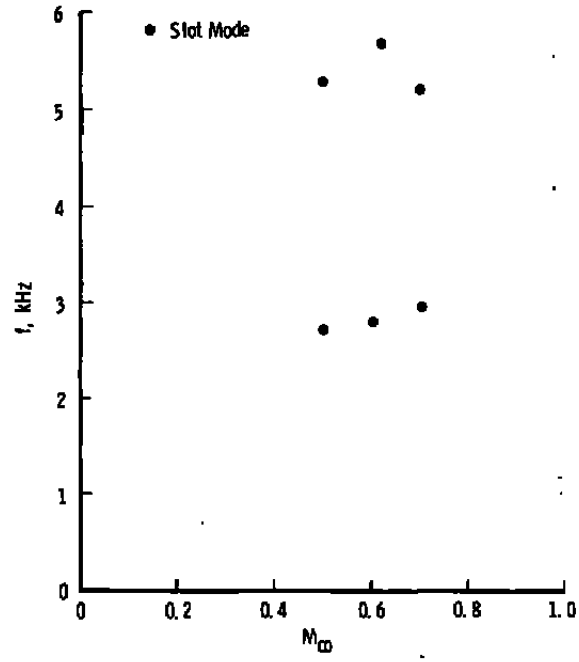

Figure 31. Predominant frequencies from full-depth "Zee" baffle slots inclined -15 deg.

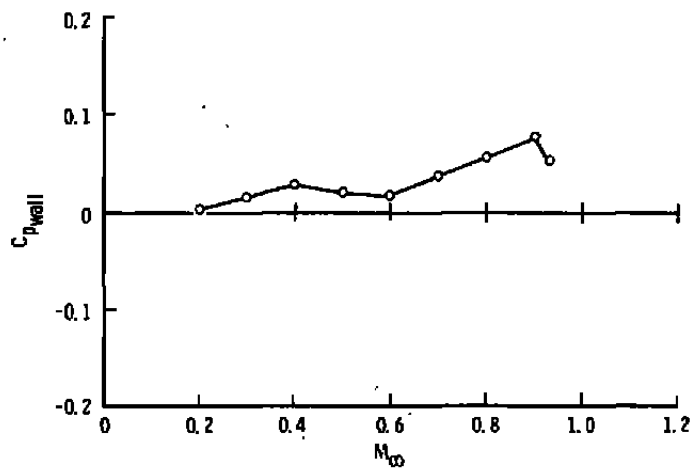

Figure 32. Wall differential pressure coefficient with full-depth "Zee" baffle slots inclined -15 deg.

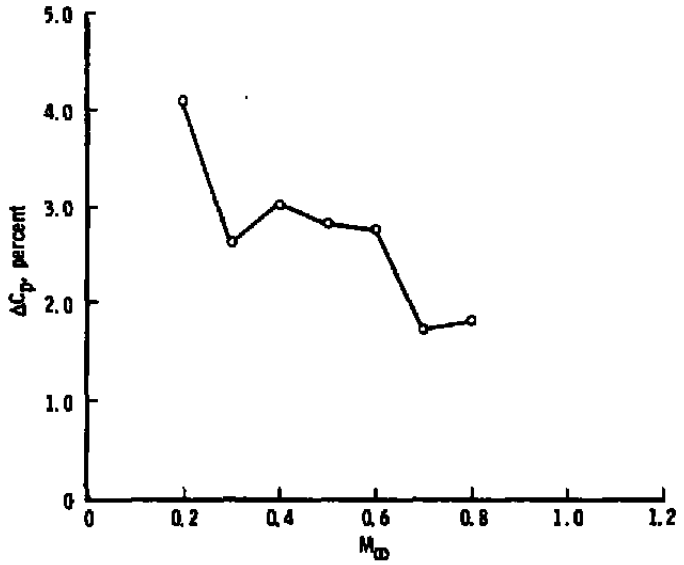

Figure 33. Noise levels from full-depth "semicircular" baffle slots inclined 60 deg.

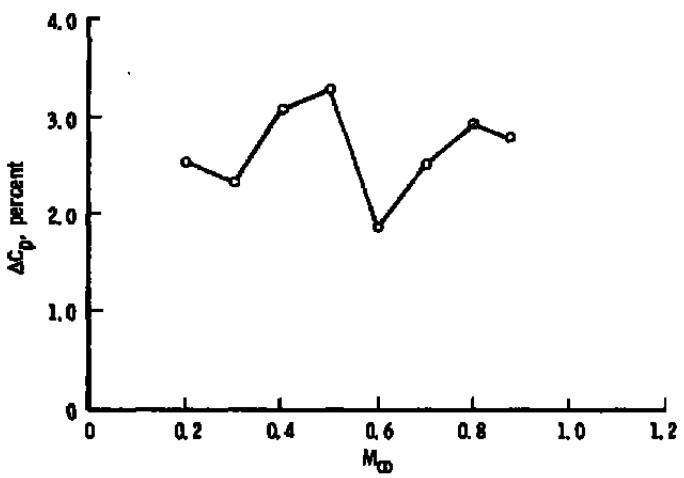

Figure 34. Noise levels from full-depth "semicircular" baffle slots inclined 45 deg.

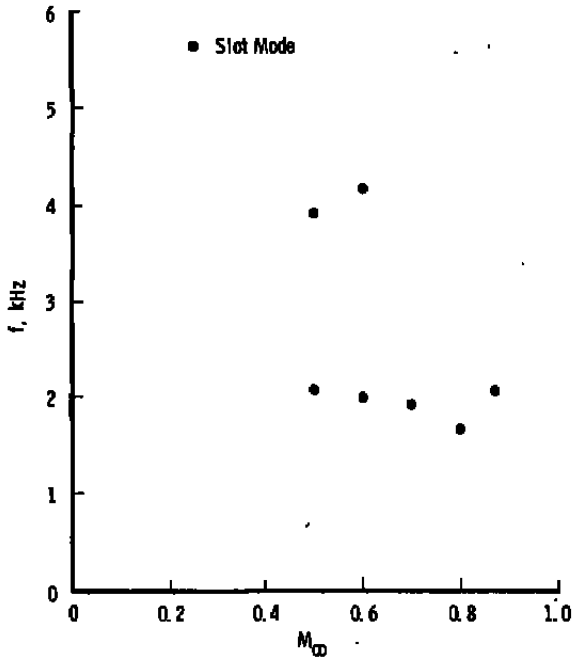

Figure 35. Predominant frequencies from full-depth "semicircular" baffle slots inclined 45 deg.

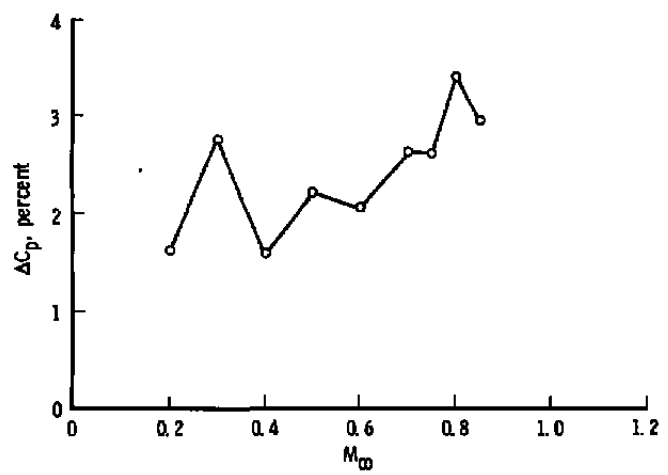

Figure 36. Noise levels from full-depth "semicircular" baffle slots inclined 30 deg.

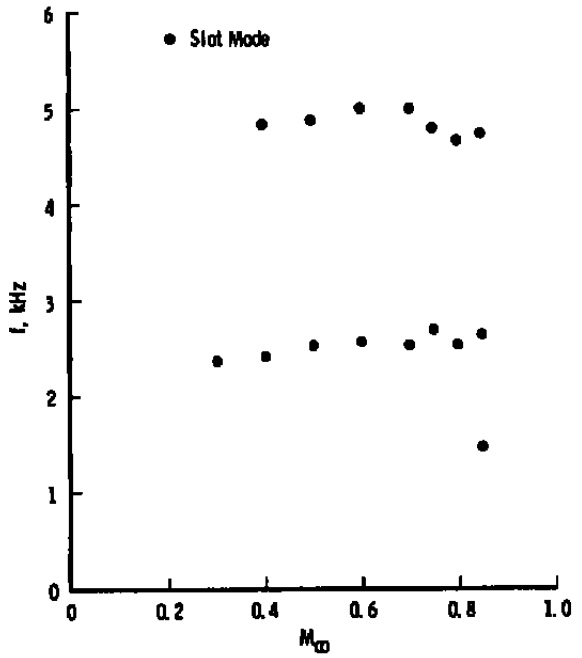

Figure 37. Predominant frequencies from full-depth "semicircular" baffle slots inclined 30 deg.

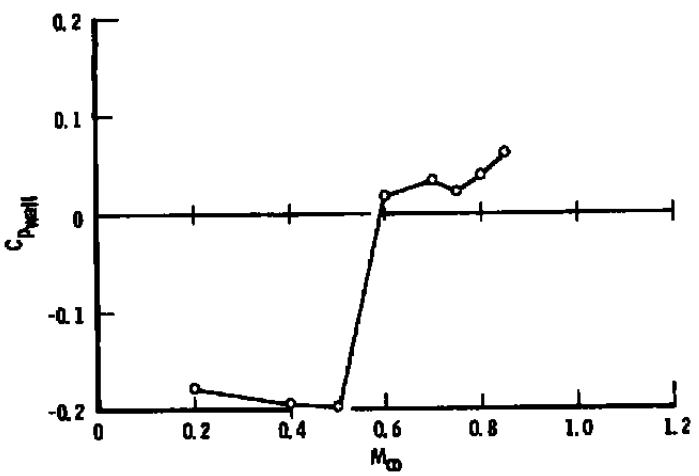

Figure 38. Wall differential pressure coefficient with full-depth "semicircular" baffle slots inclined 30 deg.

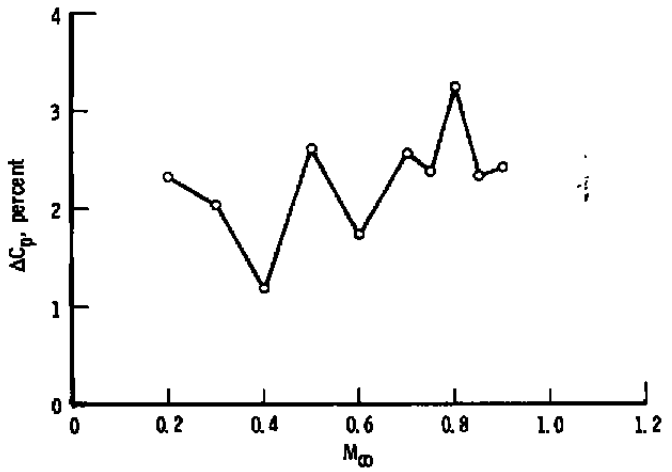

Figure 39. Noise levels from full-depth "semicircular" baffle slots inclined 15 deg.

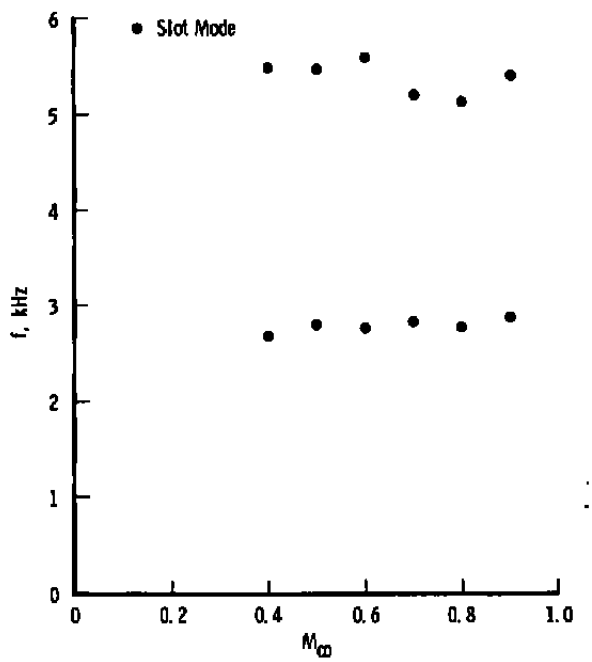

Figure 40. Predominant frequencies from full-depth "semicircular" baffle slots inclined 15 deg.

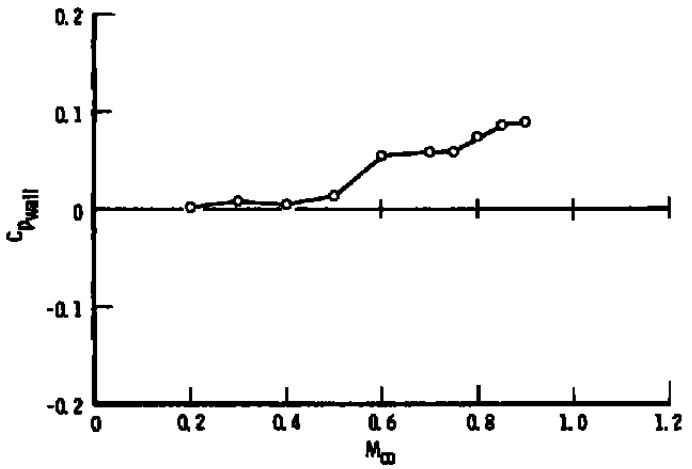

Figure 41. Wall differential pressure coefficient with full-depth "semicircular" baffle slots inclined 15 deg.

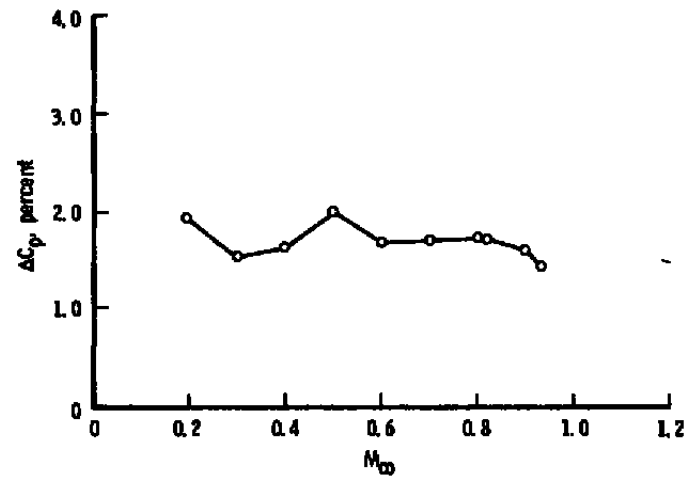

Figure 42. Noise levels from half-depth "Zee" baffle slots inclined 60 deg.

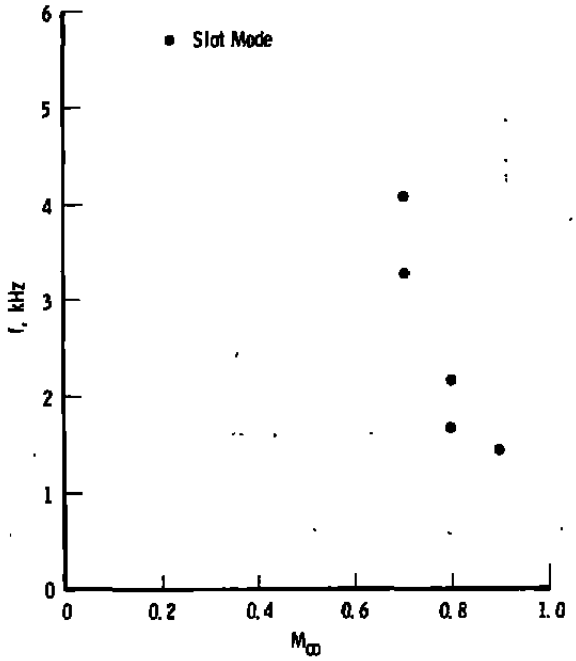

Figure 43. Predominant frequencies from half-depth "Zee" baffle slots inclined 60 deg.

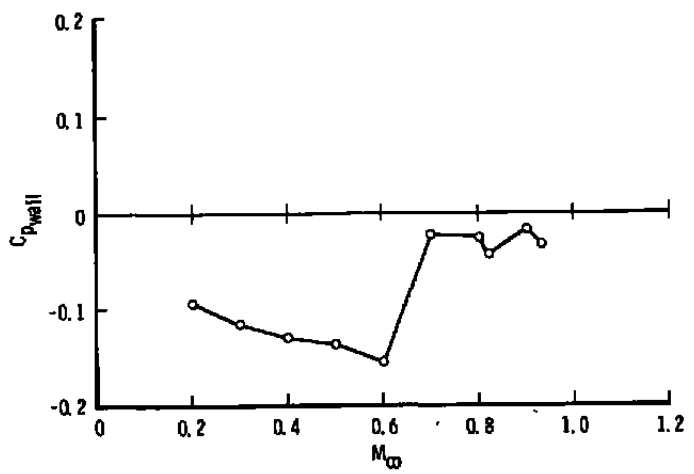

Figure 44. Wall differential pressure coefficient with half-depth "Zee" baffle slots inclined 60 deg.

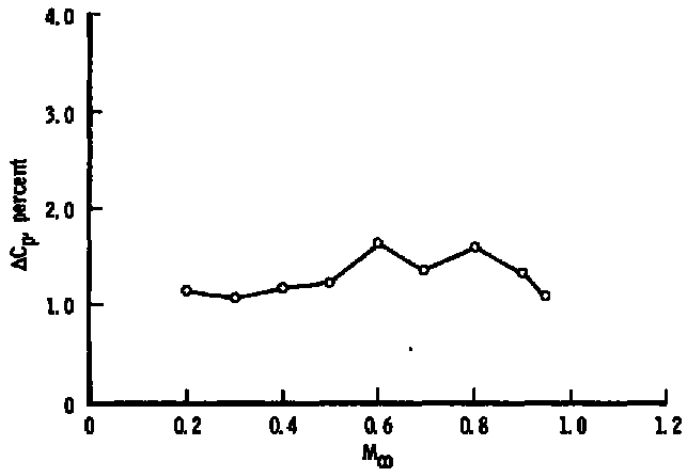

Figure 45. Noise levels from half-depth "Zee" baffle slots inclined 45 deg.

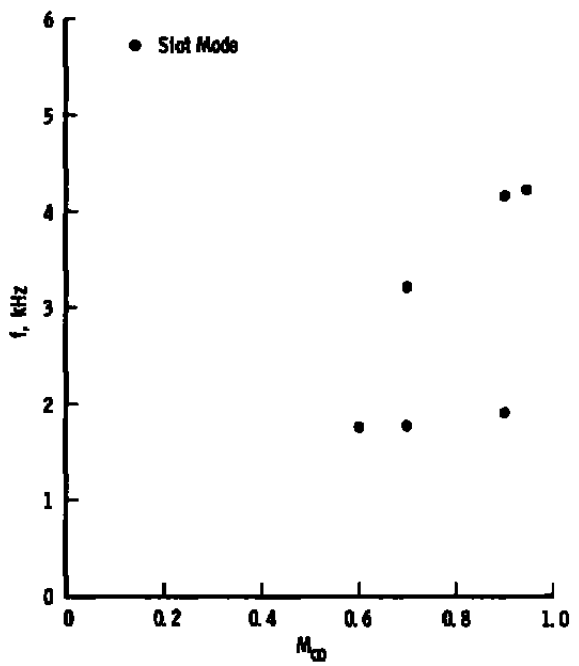

Figure 46. Predominant frequencies from half-depth "Zee" baffle slots inclined 45 deg.

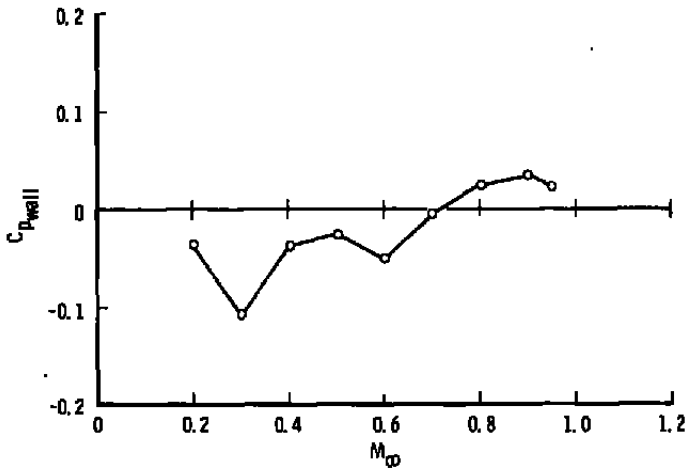

Figure 47. Wall differential pressure coefficient with half-depth "Zee" baffle slots inclined 45 deg.

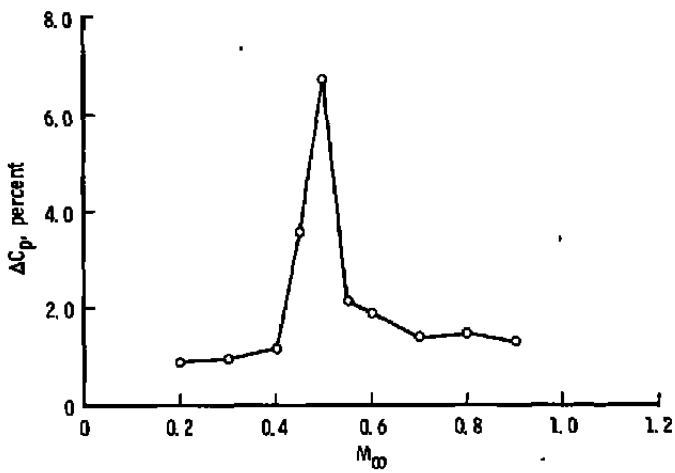

Figure 48. Noise levels from half-depth "Zee" baffle slots inclined 30 deg.

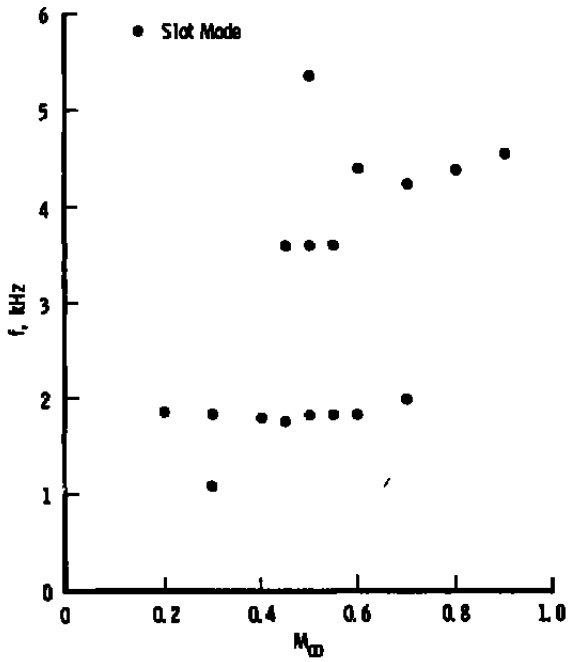

Figure 49. Predominant frequencies from half-depth "Zee" baffle slots inclined 30 deg.

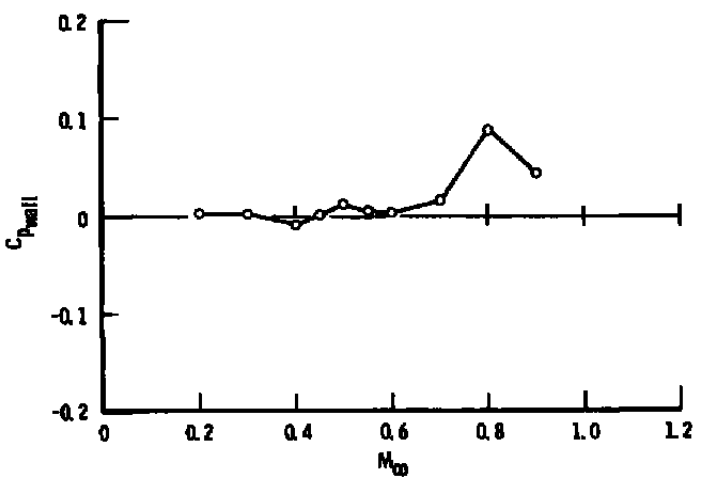

Figure 50. Wall differential pressure coefficient with half-depth "Zee" baffle slots inclined 30 deg.

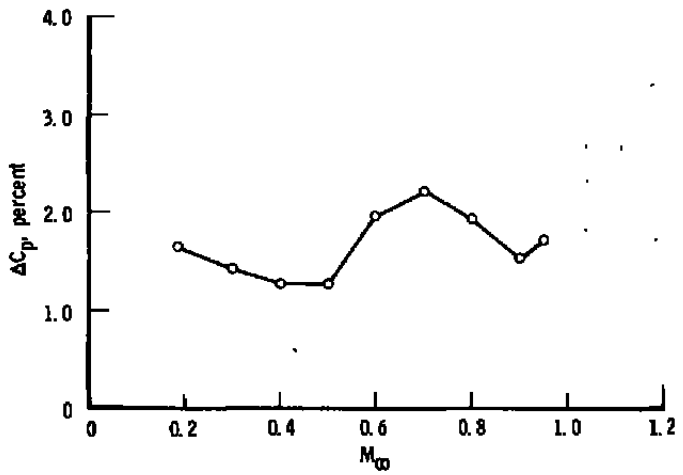

Figure 51. Noise levels from half-depth "Zee" baffle slots inclined 15 deg.

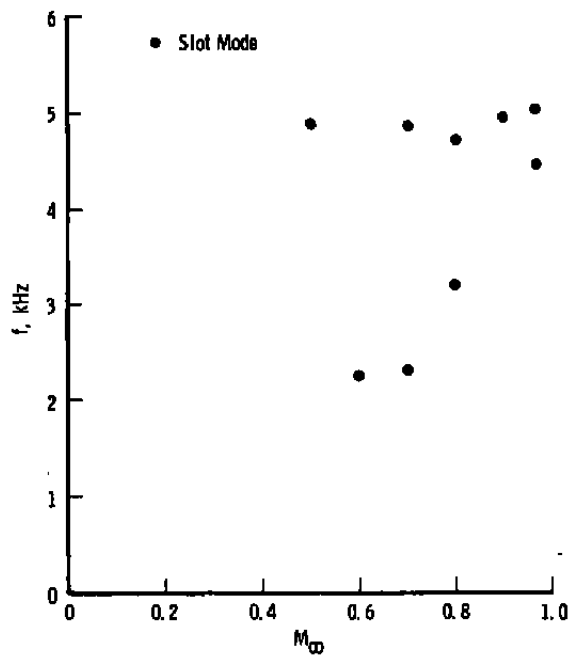

Figure 52. Predominant frequencies from half-depth "Zee" baffle slots inclined 15 deg.

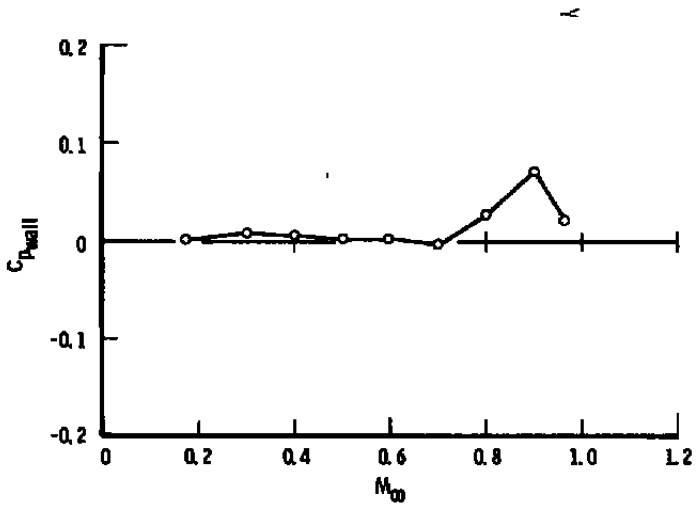

Figure 53. Wall differential pressure coefficient with half-depth "Zee" baffle slots inclined 15 deg.

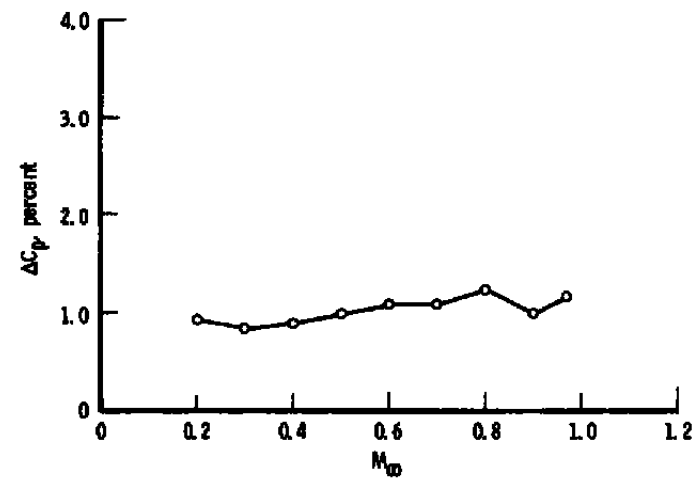

Figure 54. Noise levels from half-depth "Zee" baffle slots inclined -15 deg.

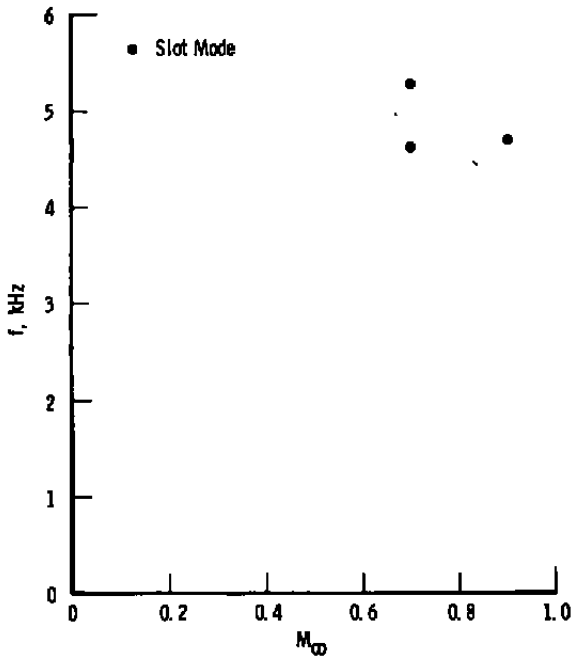

Figure 55. Predominant frequencies from half-depth "Zee" baffle slots inclined -15 deg.

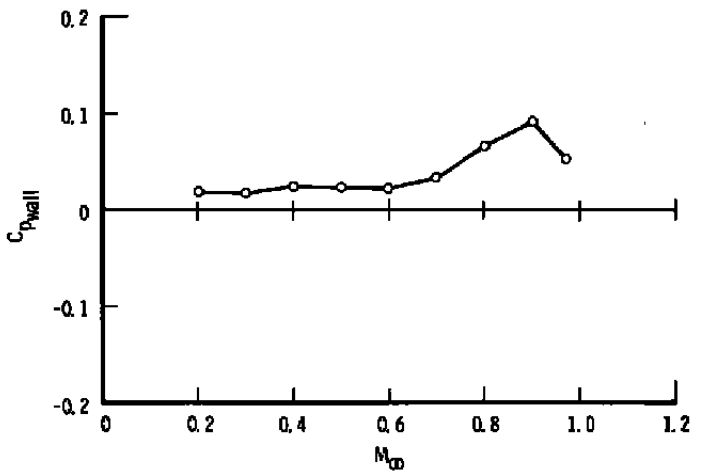

Figure 56. Wall differential pressure coefficient with half-depth. "Zee" baffle slots inclined -15 deg.

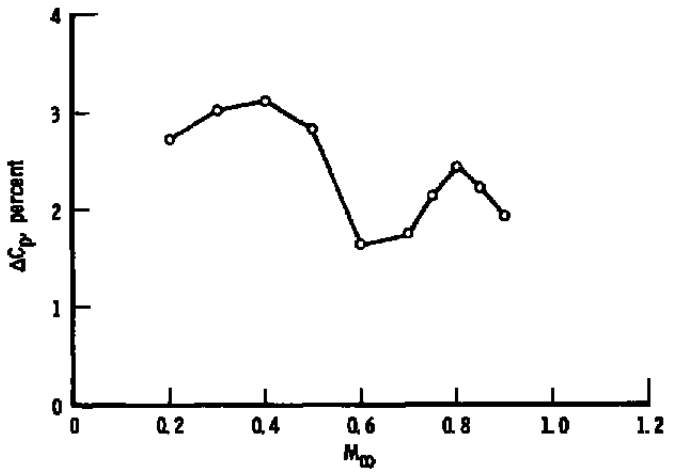

Figure 57. Noise levels from half-depth "semicircular" baffle slots inclined 60 deg.

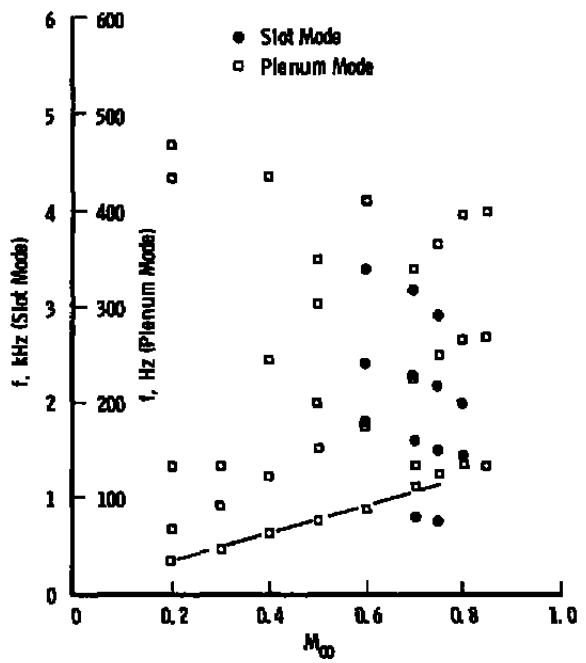

Figure 58. Predominant frequencies from half-depth "semicircular" baffle slots inclined 60 deg.

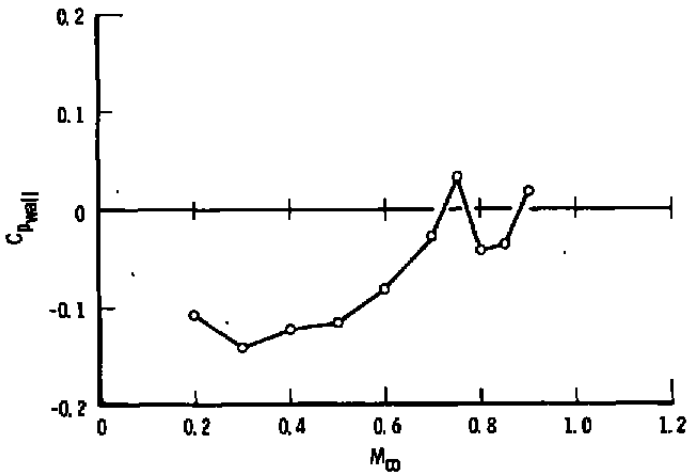

Figure 59. Wall differential pressure coefficient with half-depth "semicircular" baffle slots inclined 60 deg.

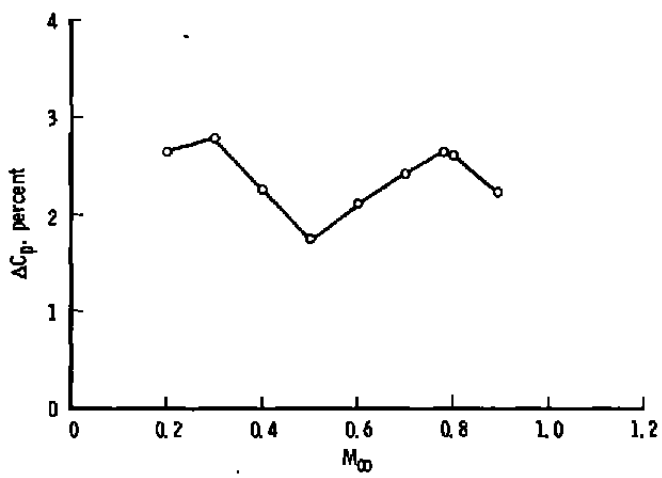

Figure 60. Noise levels from half-depth "semicircular" baffle slots inclined 45 deg.

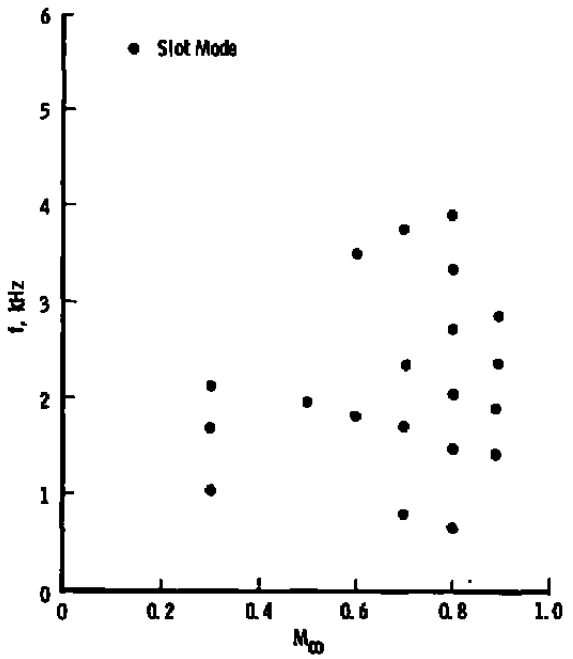

Figure 61. Predominant frequencies from half-depth "semicircular" baffle slots inclined 45 deg.

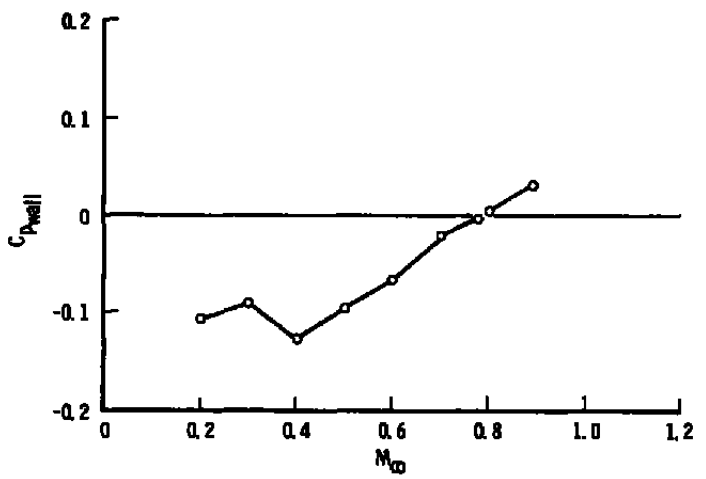

Figure 62. Wall differential pressure coefficient with half-depth semicircular" baffle slots inclined 45 deg.

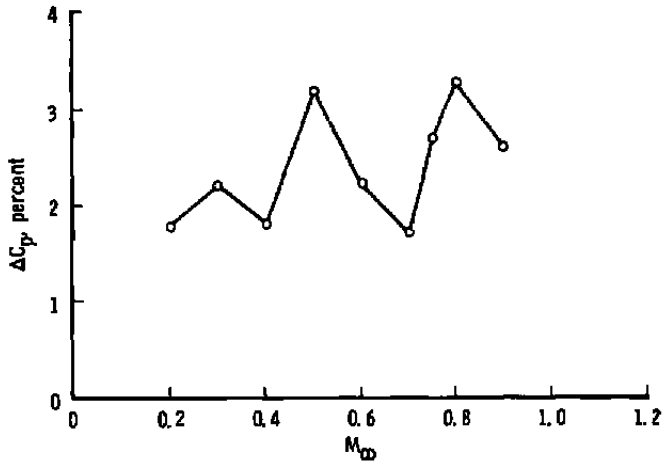

Figure 63. Noise levels from half-depth "semicircular" baffle slots inclined 30 deg.

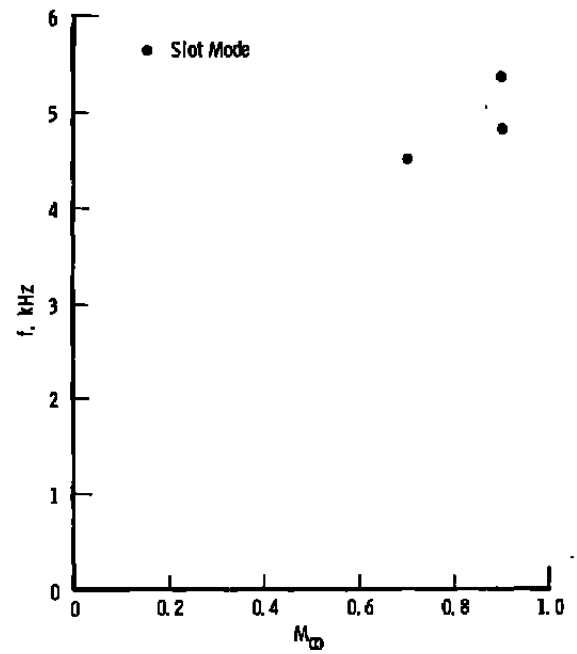

Figure 64. Predominant frequencies from half-depth "semicircular" baffle slots inclined 30 deg.

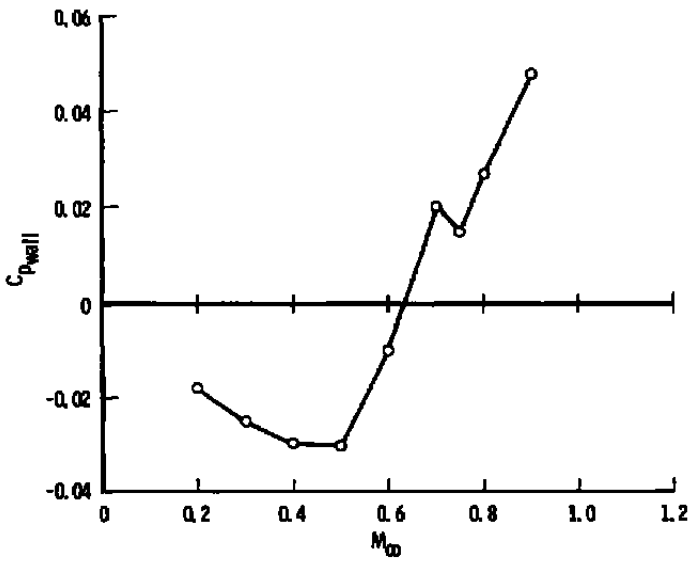

Figure 65. Wall differential pressure coefficient with half-depth "semicircular" baffle slots inclined 30 deg.

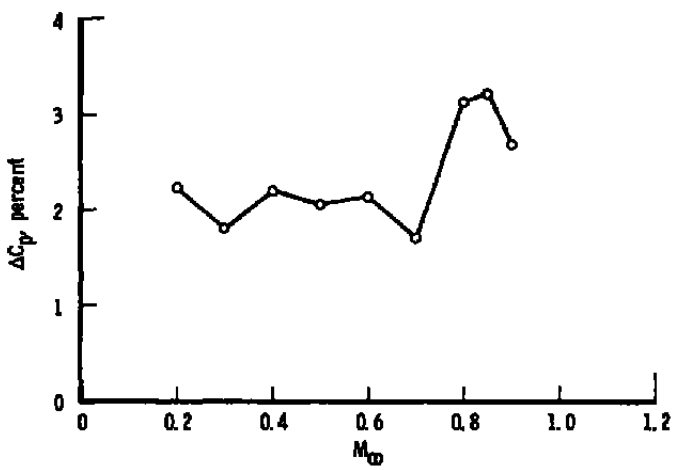

Figure 66. Noise levels from half-depth "semicircular" baffle slots inclined 15 deg.

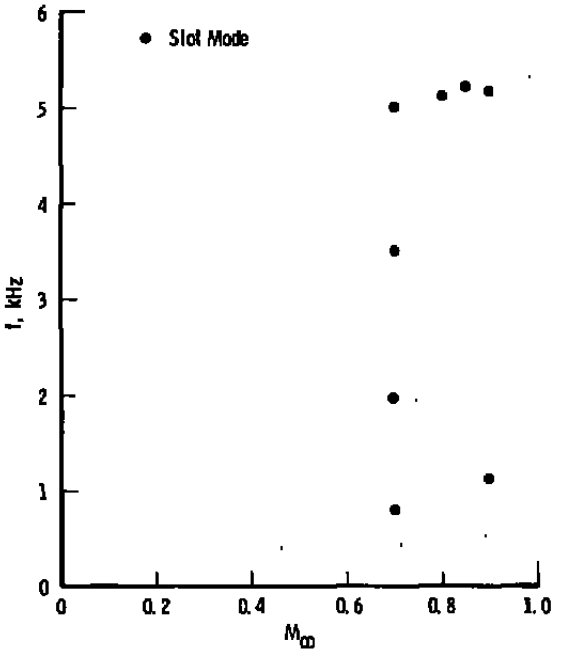

Figure 67. Predominant frequencies from half-depth "semicircular" baffle slots inclined 15 deg.

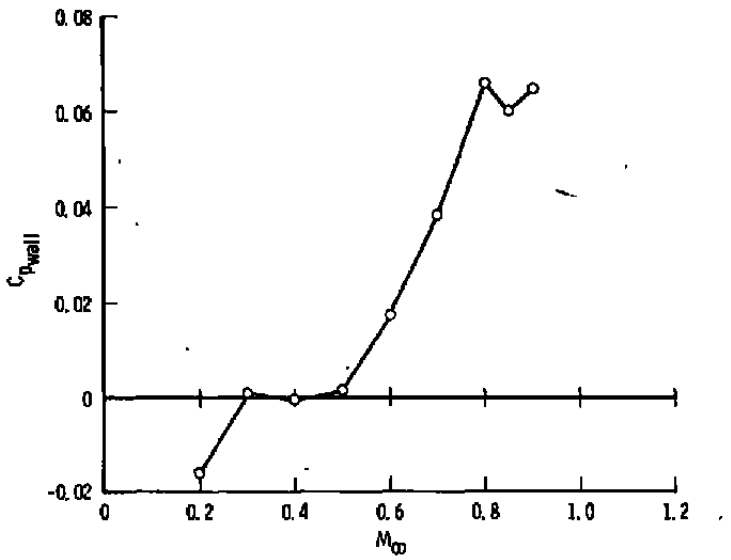

Figure 68. Wall differential pressure coefficient with half-depth "semicircular" baffle slots inclined 15 deg.

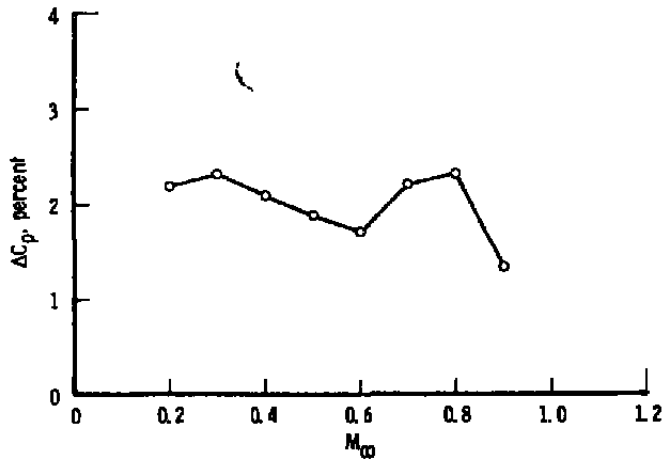

Figure 69. Noise levels from full-depth "Zee" baffles recessed and inclined 60 deg.

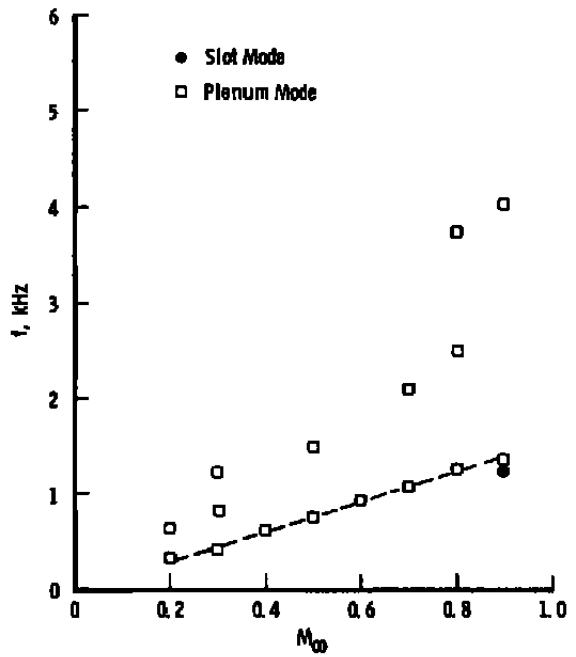

Figure 70. Predominant frequencies from full-depth "Zee" baffles recessed and inclined 60 deg.

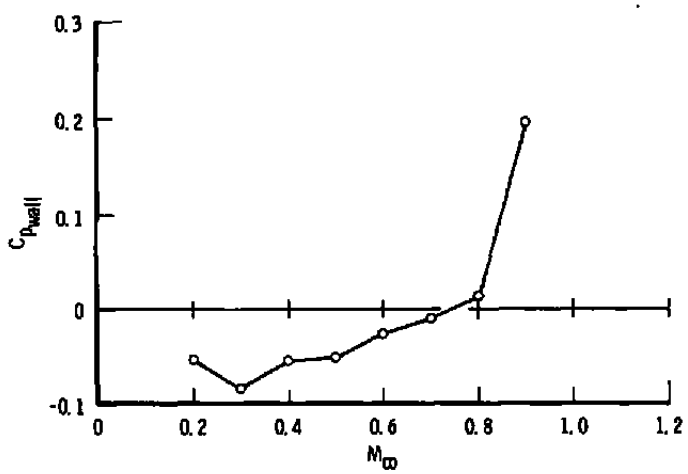

Figure 71. Wall differential pressure coefficient with full-depth "Zee" baffles recessed and inclined 60 deg.

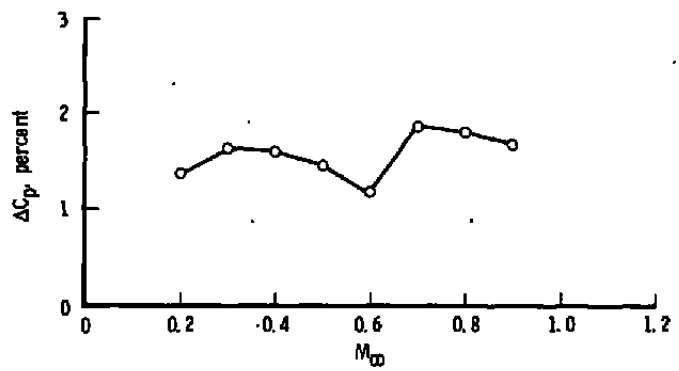

Figure 72. Noise levels from bidirectional "Zee" baffle slots.

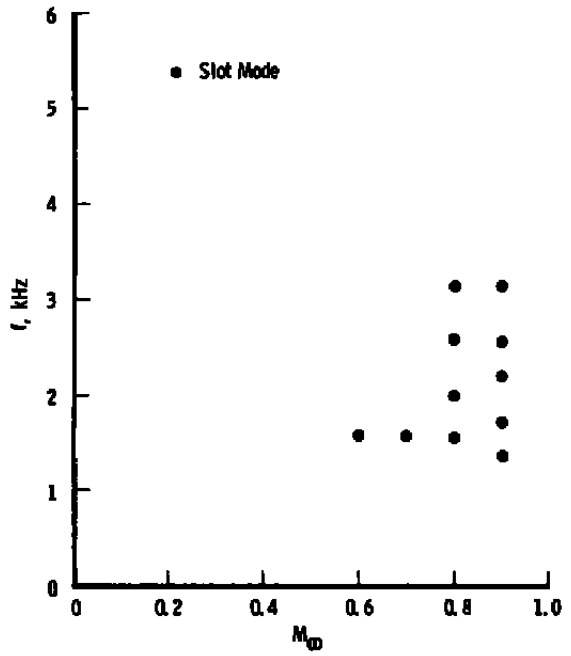

Figure 73. Predominant frequencies from bidirectional "Zee" baffle slots.

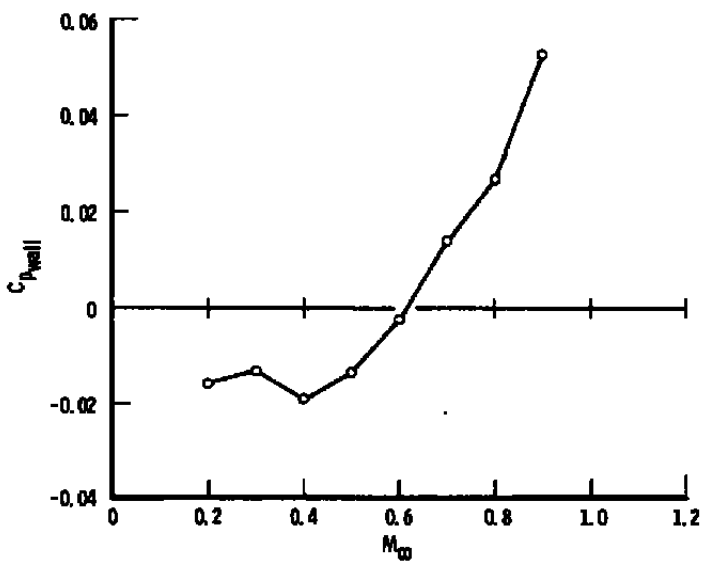

Figure 74. Wall differential pressure coefficient with half-depth Zee" baffle slots.

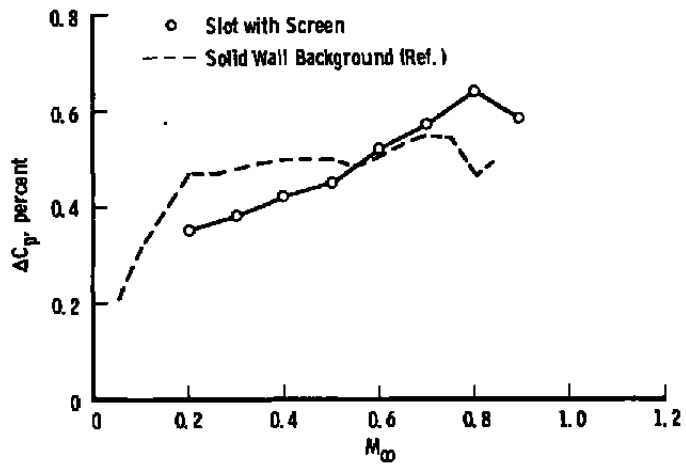

Figure 75. Noise levels from full-depth "Zee" baffle slots with wire screen overlay inclined 60 deg.

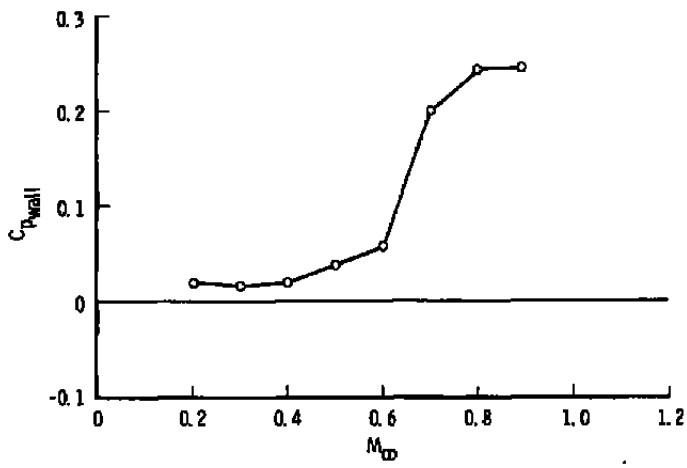

Figure 76. Wall differential pressure coefficient with full-depth "Zee" baffle slots with wire screen overlay inclined 60 deg.

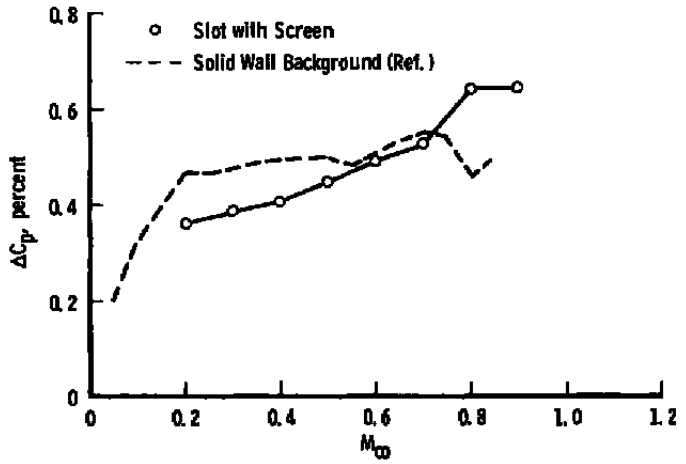

Figure 77. Noise levels from full-depth "Zee" baffle slots with wire screen overlay inclined 45 deg.

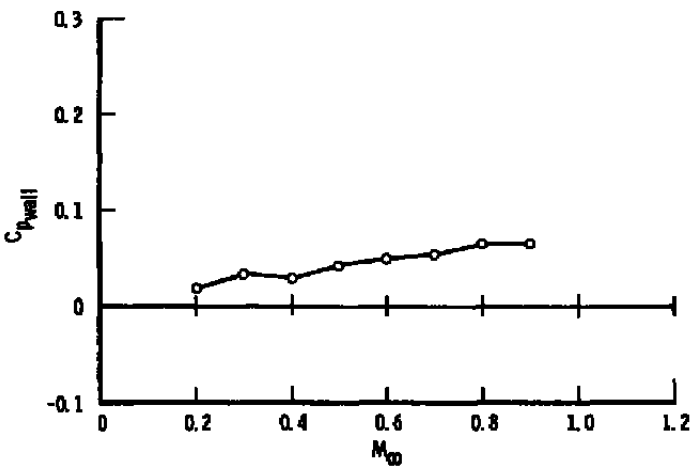

Figure 78. Wall differential pressure coefficient with full-depth "Zee" baffle slots with wire screen overlay inclined 45 deg.

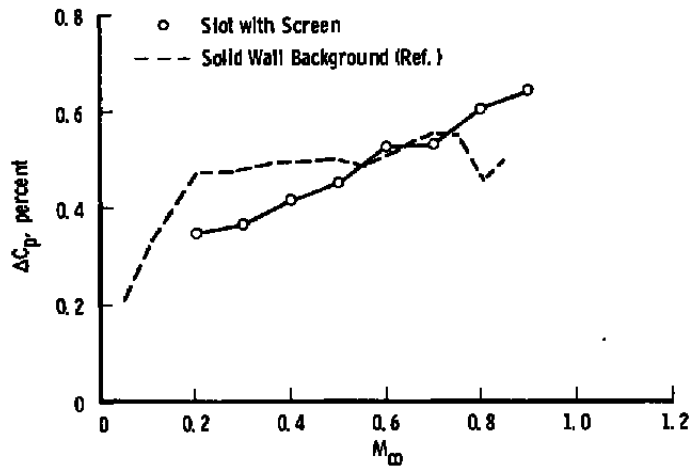

Figure 79. Noise levels from full-depth "Zee" baffle slots with wire screen overlay inclined 30 deg.

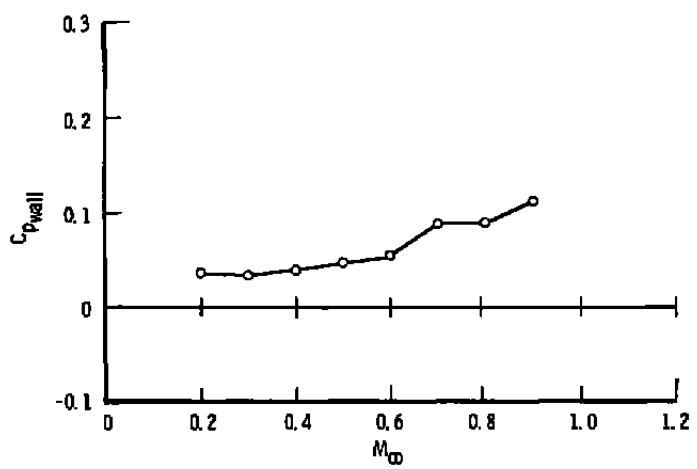

Figure 80. Wall differential pressure coefficient with full-depth "Zee" baffle slots with wire screen overlay inclined 30 deg.

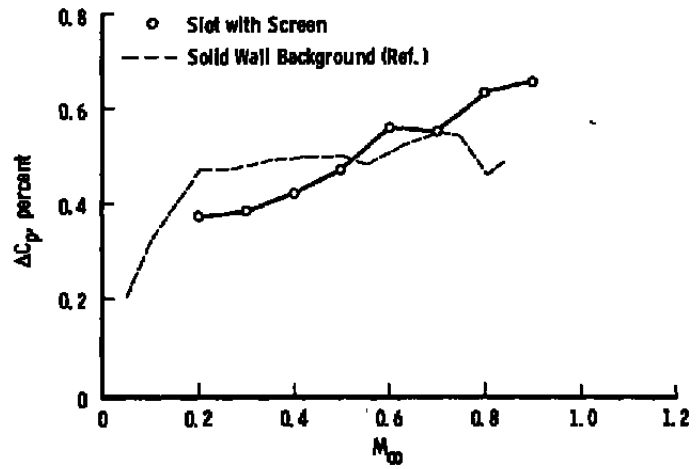

Figure 81. Noise levels from full-depth "Zee" baffle slots with wire screen overlay inclined 15 deg.

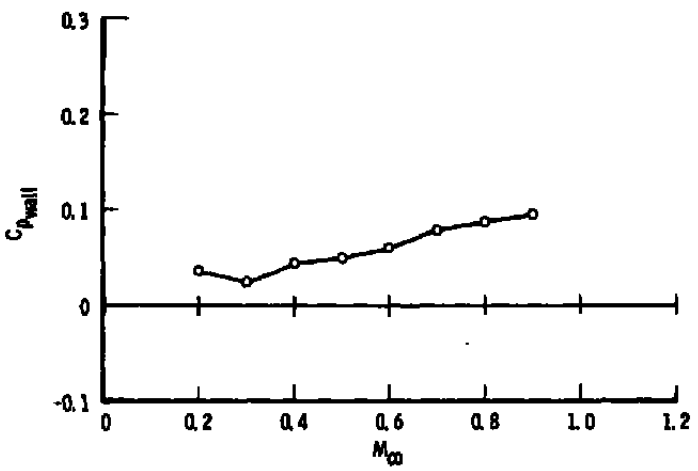

Figure 82. Wall differential pressure coefficient with full-depth "Zee" baffle slots with wire screen overlay inclined 15 deg.

Table 1. Baffle Geometry

Baffle Pattern	θ, deg	D
"Zee" and "Semicircular"	15	2.25 in. (5.64 cm)
	30	
	45	
	60	
	15	1.125 in. (2.82 cm)
	30	
	45	
	60	

Note: Standard is "Zee", θ = 0, D = 2.25 in.

Table 2. Summary of Results for Inclined Baffles

Pattern	θ, deg	D, cm	ΔC_p, percent, maximum	C_{Pwall}, maximum
Open	---	---	2.8 at M_∞ = 0.90	0.280 at M_∞ = 0.70
Solid	---	---	0.55 at M_∞ = 0.70	---
"Zee"	-15	5.64	1.4 at M_∞ = 0.60	0.076 at M_∞ = 0.90
	0*		4.0 at M_∞ = 0.75	0.038 at M_∞ = 0.99
	15		3.2 at M_∞ = 0.94	0.023 at M_∞ = 0.80
	30		3.2 at M_∞ = 0.70	0.020 at M_∞ = 0.99
	45		5.3 at M_∞ = 0.99	-0.043 at M_∞ = 1.02
	60		3.0 at M_∞ = 0.20	0.002 at M_∞ = 0.80
	-15	2.82	1.2 at M_∞ = 0.80	0.090 at M_∞ = 0.90
	15		2.2 at M_∞ = 0.70	0.070 at M_∞ = 0.90
	30		6.7 at M_∞ = 0.50	0.086 at M_∞ = 0.80
	45		1.6 at M_∞ = 0.60	0.033 at M_∞ = 0.90
	60		2.0 at M_∞ = 0.50	-0.018 at M_∞ = 0.90
"Semicircular"	15	5.64	3.2 at M_∞ = 0.80	0.088 at M_∞ = 0.90
	30		3.4 at M_∞ = 0.80	0.061 at M_∞ = 0.85
	45		3.3 at M_∞ = 0.50	---
	60		4.1 at M_∞ = 0.20	---
	15	2.82	3.2 at M_∞ = 0.85	0.066 at M_∞ = 0.80
	30		3.3 at M_∞ = 0.80	0.048 at M_∞ = 0.90
	45		2.8 at M_∞ = 0.30	0.031 at M_∞ = 0.89
	60		3.1 at M_∞ = 0.40	0.032 at M_∞ = 0.75
"Zee" with Screen	0	5.64	2.40 at M_∞ = 0.75	0.032 at M_∞ = 1.00
	15		0.66 at M_∞ = 0.90	0.093 at M_∞ = 0.90
	30		0.65 at M_∞ = 0.90	0.11 at M_∞ = 0.90
	45		0.64 at M_∞ = 0.90	0.064 at M_∞ = 0.90
	60		0.64 at M_∞ = 0.80	0.25 at M_∞ = 0.89
"Zee" Recessed 1/4" below Surface	60	5.64	2.3 at M_∞ = 0.30	0.20 at M_∞ = 0.90
"Zee" with Bidirectional Baffle	45 and 30	5.64	1.9 at M_∞ = 0.70	0.053 at M_∞ = 0.90

*Ames 11- by 11-foot Wind Tunnel Configuration (Standard)

NOMENCLATURE

ΔC_p	Fluctuating pressure coefficient ($\tilde{p}_{rms}/q_\infty$), percent
$C_{p_{wall}}$	Wall differential pressure coefficient
D	Baffle depth dimension
f	Frequency, Hz
M_∞	Free-stream Mach number in the test section
p_c	Plenum chamber static pressure
p_s	Reference test section sidewall static pressure
p_t	Tunnel total pressure
$p'(t)$	Instantaneous fluctuating pressure level in the test section
$\tilde{p}_{rms}$	Root-mean-square fluctuating pressure level in the test section
q_∞	Free-stream dynamic pressure in the test section
R	"Semicircular" baffle characteristic radius
t	Baffle web thickness
T	Averaging time, sec
γ	Ratio of specific heats, 1.4 for air
θ	Baffle web inclination angle, deg